https://doi.org/10.1093/plcell/koac357 THE PLANT CELL 2023: 35: 673–699

THE PLANT CELL

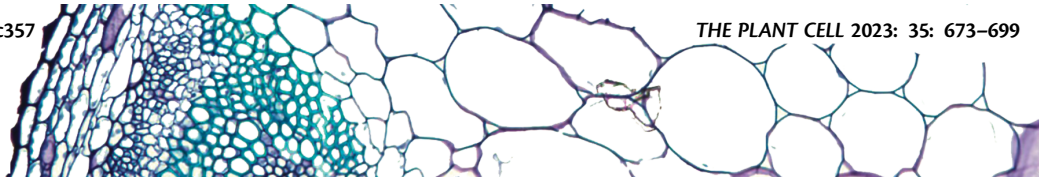

Research Article

Analyses of Cullin1 homologs reveal functional redundancy in S-RNase-based self-incompatibility and evolutionary relationships in eudicots

Linhan Sun,[1] **Shiyun Cao**,[2] **Ning Zheng**[2] **and Teh-hui Kao**[1,3,*]

1 Intercollege Graduate Degree Program in Plant Biology, The Pennsylvania State University, University Park, Pennsylvania 16802, USA
2 Howard Hughes Medical Institute, Department of Pharmacology, University of Washington, Seattle, Washington 98195, USA
3 Department of Biochemistry and Molecular Biology, The Pennsylvania State University, University Park, Pennsylvania 16802, USA

*Author for correspondence: txk3@psu.edu
The author responsible for distribution of materials integral to the findings presented in this article, in accordance to the policy described in the Instructions for Authors (https://academic.oup.com/plcell/pages/General-Instructions), is Teh-hui Kao (txk3@psu.edu).

Abstract

In *Petunia* (Solanaceae family), self-incompatibility (SI) is regulated by the polymorphic *S*-locus, which contains the pistil-specific *S-RNase* and multiple pollen-specific *S-Locus F-box* (*SLF*) genes. SLFs assemble into E3 ubiquitin ligase complexes known as Skp1–Cullin1–F-box complexes (SCF^{SLF}). In pollen tubes, these complexes collectively mediate ubiquitination and degradation of all nonself S-RNases, but not self S-RNase, resulting in cross-compatible, but self-incompatible, pollination. Using *Petunia inflata*, we show that two pollen-expressed Cullin1 (CUL1) proteins, PiCUL1-P and PiCUL1-B, function redundantly in SI. This redundancy is lost in *Petunia hybrida*, not because of the inability of PhCUL1-B to interact with SSK1, but due to a reduction in the *PhCUL1-B* transcript level. This is possibly caused by the presence of a DNA transposon in the *PhCUL1-B* promoter region, which was inherited from *Petunia axillaris*, one of the parental species of *Pe. hybrida*. Phylogenetic and syntenic analyses of *Cullin* genes in various eudicots show that three Solanaceae-specific *CUL1* genes share a common origin, with *CUL1-P* dedicated to S-RNase-related reproductive processes. However, *CUL1-B* is a dispersed duplicate of *CUL1-P* present only in *Petunia*, and not in the other species of the Solanaceae family examined. We suggest that the *CUL1*s involved (or potentially involved) in the SI response in eudicots share a common origin.

IN A NUTSHELL

Background: For any organism, inbreeding reduces fitness of the progeny. To prevent inbreeding, plants have adopted a reproductive strategy, self-incompatibility, to allow pistils to reject genetically identical self-pollen and accept nonself pollen for fertilization. In eudicot families, such as the Solanaceae, Plantaginaceae, and Rosaceae, the pistil uses a cytotoxic protein, S-RNase, to inhibit growth of self-pollen tubes. Nonself pollen overcomes S-RNase cytotoxicity using a suite of S-locus F-box (SLF) proteins to mediate degradation of nonself S-RNases. Each SLF is a component of a protein complex, SCF^{SLF}. In *Petunia inflata* (Solanaceae), this complex contains two pollen-specific components, PiSSK1 and PiCUL1-P.

Question: We wished to determine whether PiCUL1-P is essential for pollen to detoxify nonself S-RNases during cross-compatible pollination, and whether PiCUL1-P functions specifically in self-incompatibility. We also wanted to examine the identity of CUL1 proteins potentially involved in S-RNase-based self-incompatibility in other eudicot families.

Received September 19, 2022. Accepted December 05, 2022. Advance access publication December 8, 2022

Findings: Using CRISPR/Cas9-mediated gene knockout, we found that, in *Pe. inflata*, pollen lacking functional PiCUL1-P could still detoxify nonself S-RNases during cross-compatible pollination, whereas pollen lacking both PiCUL1-P and another CUL1, PiCUL1-B, could not, suggesting functional redundancy of these two CUL1 proteins. In *Petunia hybrida*, we found a transposable element inserted in the promoter region of *CUL1-B*, which might result in drastic reduction of its transcript level, rendering PhCUL1-P essential for cross-compatibility. We did not find *CUL1-B* in the other Solanaceae species examined. Analyses of *CUL1* evolution in eudicots revealed that all CUL1s involved, or potentially involved, in self-incompatibility possibly share a common ancestor.

Next steps: At the biochemical level, we want to determine the amino acids of *Petunia* CUL1-P and CUL1-B that are responsible for their specific interactions with SSK1 to form SCF^{SLF} complexes. At the evolutionary level, we want to investigate whether the CUL1 and SSK1 components of SCF^{SLF} complexes might have co-evolved in eudicots.

Introduction

Most flowering plants produce bisexual flowers, with the anthers and the pistil located in the same flower. The proximity of the male and female reproductive organs creates a strong tendency to self-pollinate, which, if successful in the long term, results in inbreeding and consequent reduced fitness in the progeny plus decreased genetic diversity in the species. As plants cannot move about to select mates, many flowering plants have evolved and adapted a variety of strategies to prevent self-fertilization and promote out-crossing, including dioecy (male and female flowers are on separate plants), dichogamy (anthers and stigma mature at different times during development), and self-incompatibility (SI; the inability to self-pollinate). SI is first classified into heteromorphic and homomorphic types: in heteromorphic types, male and female plants of the same species have different flower morphologies, whereas for the homomorphic type, they have the same morphology (de Nettancourt, 2001).

This work deals with the homomorphic SI, specifically, a type of mechanism that has been reported to be present in several eudicot families, including the Solanaceae, Plantaginaceae, Rosaceae, and Rutaceae (Fujii et al., 2016; Liang et al., 2020). In all these families, the outcome of pollen–pistil interactions, i.e. rejection of self-pollen and acceptance of nonself pollen by the pistil, is determined by a single polymorphic locus, termed the *S*-locus. Variants (haplotypes) at this locus are designated S_1, S_2, S_3, etc. If the same *S*-haplotype found in pollen is also carried by a pistil, the pistil recognizes the pollen as self-pollen and inhibits pollen tube growth in the upper part of the style. If the *S*-haplotype of pollen is different from both *S*-haplotypes of a pistil, the pistil recognizes the pollen as nonself pollen and allows pollen tubes to grow down to the ovary to effect fertilization (de Nettancourt, 2001).

In pistils of *Petunia*, a member of the Solanaceae family, the determinant for SI is the polymorphic *S-RNase* gene, which encodes a secreted ribonuclease (Huang et al., 1994; Lee et al., 1994; Murfett et al., 1994). The pollen determinant for SI is encoded by multiple *S-locus F-box* (*SLF*) genes, with the number of *SLF*s ranging from 16 to 20 depending on the specific *S*-haplotype (Kubo et al., 2010; Williams et al., 2014a; Kubo et al., 2015; Wu et al., 2020). Each SLF possesses an F-box motif at its N-terminus. A conventional F-box protein serves as the substrate binding subunit of the Skp1–Cullin1–F-box (SCF)-type complex, a multi-subunit E3 ubiquitin ligase (Zheng et al., 2002). In conjunction with ubiquitin-activating enzyme E1 and ubiquitin-conjugating enzyme E2, it catalyzes transfer of polyubiquitin chain(s) to the protein substrates for subsequent degradation by the 26S proteasome. *SLF1* was identified in *Pe. inflata* based on the results of an in vivo function assay showing that expression of its S_2-allele, S_2-*SLF1*, in S_1 and S_3 transgenic pollen abolished SI (Sijacic et al., 2004). These results are consistent with the prediction resulting from the observation that, in *Petunia*, SI broke down in diploid pollen carrying two different *S*-haplotypes (Stout and Chandler, 1941; Stout and Chandler, 1942; Brewbaker and Natarajan, 1960). A biochemical interpretation of these results is that, as an S_1 (or S_3) transgenic pollen tube is growing in an S_1-carrying pistil (or an S_3-carrying pistil), S_1-RNase (or S_3-RNase) taken up into the transgenic pollen tube cannot act because S_2-SLF1 produced in the S_1 transgenic pollen tube (or S_3 transgenic pollen tube) interacts with S_1-RNase (or S_3-RNase) to mediate its ubiquitination and degradation (Sijacic et al., 2004).

After a pollen tube has grown from the stigma into the style, both self and nonself S-RNases are taken up by the pollen tube (Luu et al., 2000; Goldraij et al., 2006); however, only self S-RNase can inhibit pollen tube growth (Huang et al., 1994). A model named collaborative nonself recognition has been proposed to explain how multiple SLF proteins produced by the pollen tube of a given *S*-haplotype allow only their self S-RNase to function inside the pollen tube (Kubo et al., 2010). This model proposes that each SLF can interact only with a subset of its nonself S-RNases to mediate their ubiquitination and degradation, but all SLFs can collectively interact with, and induce degradation of, all their nonself S-RNases. This model further proposes that none of the SLFs can interact with its self S-RNase. Thus, even though both self and nonself S-RNases can enter a pollen tube, only self S-RNase can degrade pollen tube RNAs, resulting in SI.

The in vivo functional assay mentioned above has been used to establish interaction relationships between SLFs and S-RNases in *Petunia* (Sijacic et al., 2004; Hua et al., 2007; Kubo et al., 2010; Sun and Kao, 2013; Williams et al., 2014b; Kubo et al., 2015; Sun et al., 2018; Wu et al., 2018), and the results are consistent with this model. For example, in *Pe. inflata*, none of the 17 SLF proteins produced by S_2 pollen can interact with their self S-RNase, S_2-RNase (Hua et al.,

2007; Sun and Kao, 2013; Williams et al., 2014b; Sun et al., 2018). Moreover, the genetically determined relationships between these 17 SLF proteins and S-RNases have been verified by CRISPR (clustered regularly interspaced short palindromic repeats)/Cas9 (CRISPR-associated protein 9)-mediated knockout of S_2-*SLF1* (Sun et al., 2018). For example, according to the results of the in vivo functional assay, S_2-SLF1 is the only SLF produced by S_2 pollen that can interact with and inhibit S_3-RNase. Indeed, knocking out S_2-SLF1 resulted in S_2 pollen that was completely incompatible with normally compatible S_3-carrying pistils (Sun et al., 2018).

In addition to an F-box protein, a conventional SCF-type E3 ligase complex also contains Cullin1 (CUL1), a scaffold protein that interacts with Rbx1 (a RING-box protein that recruits E2 ubiquitin-conjugating enzyme) on one end, and the F-box protein on the other end via an adaptor protein Skp1 (Zheng et al., 2002). In *Pe. inflata*, we previously used co-immunoprecipitation (Co-IP) assays and mass spectrometry (MS) to show that green fluorescent protein (GFP)-fused S_2-SLF1 co-immunoprecipitated with a Skp1-like protein (PiSSK1), a CUL1 protein (PiCUL1-P), and a conventional Rbx1 protein (PiRBX1; Li et al., 2014). Further Co-IP/MS experiments, using GFP- and FLAG-fused PiSSK1 as bait, revealed that all 17 SLF proteins produced by S_2 or S_3 pollen could be assembled into similar SCF^{SLF} complexes. In addition, Co-IP/MS using Myc-tagged PiCUL1-P as bait showed that it co-immunoprecipitated with PiSSK1, PiRBX1, and an SLF protein (Li et al., 2016).

Similar SCF complex subunits were also identified in SCF^{SLF} complexes containing *Petunia hybrida* S_{3L}-SLF1 (Entani et al., 2014) or S_7-SLF2 (Liu et al., 2014). Interestingly, like *SLF*, both *Petunia SSK1* and *CUL1-P* are specifically expressed in pollen, suggesting that both genes might have evolved to function specifically in SI (Zhao et al., 2010; Li et al., 2014; Kubo et al., 2016). Indeed, for *PiSSK1*, we previously used CRISPR/Cas9 to generate its knockout mutants, and found that S_2 and S_3 pollen carrying frameshift indel alleles of *PiSSK1* were rejected by normally compatible pistils, but remained compatible with the pistils of a transgenic S_3S_3 plant that produced very little S_3-RNase due to expression of an antisense *S_3-RNase* gene (Sun and Kao, 2018). These results suggest both that PiSSK1 is essential for the ability of SLF proteins to mediate ubiquitination and degradation of non-self S-RNases for cross-compatible pollination, and that PiSSK1 is the only Skp1-like protein in pollen of *Pe. inflata* that can serve as the Skp1 subunit of SCF^{SLF} complexes (Sun and Kao, 2018). To examine the role of CUL1-P of *Pe. hybrida* (PhCUL1-P) in SI, Kubo et al. (2016) used artificial microRNA (amiRNA) to specifically knockdown the transcript level of *PhCUL1-P*, and found that, when crossed with normally compatible pistils, transmission of the single copy *ami-RNA-PhCUL1-P* (*amiCUL1-P*) transgene to progeny, via pollen, was significantly <50%. This suggests that, in *Pe. hybrida*, only PhCUL1-P is required for cross-compatible pollination.

In this work, we used in vitro protein complex reconstitution and in vivo Co-IP experiments, and found that, in *Pe. inflata*, both PiCUL1-P and another pollen-expressed CUL1 (PiCUL1-B), could serve as the CUL1 subunit of SCF^{SLF} complexes. To assess the biological function of *PiCUL1-P* and *PiCUL1-B* in SI, we used CRISPR/Cas9-mediated genome editing to separately knockout *PiCUL1-P* and *PiCUL1-B*. We then generated double knockout plants of both *PiCUL1-P* and *PiCUL1-B* and found that pollen of only the double knockout plants, but not pollen of single knockout plants of either *PiCUL1-P* or *PiCUL1-B*, was rejected by normally compatible pistils. This observation is in contrast with the result by Kubo et al. (2016) that in *Pe. hybrida*, only *PhCUL1-P* is involved in cross-compatibility.

We further showed that Myc-tagged CUL1-B of *Pe. hybrida* (PhCUL1-B) co-immunoprecipitated with FLAG- and GFP-tagged SSK1 of both *Pe. hybrida* and *Pe. inflata* in double transgenic plants, suggesting that the observed lack of redundancy of CUL1-B and CUL1-P in *Pe. hybrida* is not due to the inability of PhCUL1-B to interact with SSK1 to form SCF^{SLF} complexes. Instead, we found that the loss of redundancy in *Pe. hybrida*, a horticultural species, was likely due to the low *PhCUL1-B* transcript level. This was possibly caused by the presence of a DNA transposon sequence in the promoter region of *PhCUL1-B* that was inherited from *Petunia axillaris* (in the long-tube cade of *Petunia*), one of the parental species of *Pe. hybrida*. Interestingly, *CUL1-B* is absent in the crown-group clade (the $x = 12$ clade that includes *Solanum*, *Nicotiana*, and *Capsicum*) of the Solanaceae (Olmstead et al., 2008; Särkinen et al., 2013; Bombarely et al., 2016), whereas *CUL1-P* orthologs are present in all the Solanaceae genomes we analyzed. Finally, based on phylogenetic and syntenic analyses of *Cullin* in eudicots, we discuss the possible origin of *CUL1-P* in the Solanaceae, and the possible common origin of the *CUL1*s that are involved, or potentially involved, in S-RNase-based SI in eudicots.

Results

Both PiCUL1-P and PiCUL1-B are capable of serving as the CUL1 subunit of SCF^{SLF} complexes

The genome of *Pe. inflata* contains five *CUL1* genes, known as *CUL1-B*, *-C*, *-E*, *-G*, and *-P* (Supplemental Table S1; Hua and Kao, 2006). Among these five *CUL1*s, *PiCUL1-B* shares the highest degree of sequence similarity with *PiCUL1-P*, with 94.4% identity between their coding sequences, and 94.5% identity in their deduced amino acid sequences. This high degree of sequence similarity between PiCUL1-P and PiCUL1-B led us to hypothesize that both PiCUL1-P and PiCUL1-B can form SCF complexes by interacting with PiSSK1, the sole Skp1 subunit of SCF^{SLF} complexes (Sun and Kao, 2018). Therefore, we first assessed whether both PiCUL1-P and PiCUL1-B could interact with PiSSK1 in vivo and in vitro (Figure 1).

To examine the interactions in vivo, we made a transgene construct containing the pollen-specific *LAT52* promoter of tomato (*Solanum lycopersicum*), $LAT52_{pro}$ (Twell et al., 1990; Li et al., 2016) driving the expression of Myc:PiCUL1-B

(Supplemental Figure S1A). We then introduced the construct into *Pe. inflata* plants of S_2S_3 genotype. We then crossed one of the resulting transgenic plants with a previously generated transgenic S_2S_3 plant carrying the *LAT52*$_{pro}$*:PiSSK1:FLAG:GFP* transgene (Li et al., 2014; Supplemental Figure S1B) to generate doubly transgenic plants expressing both Myc:PiCUL1-B and PiSSK1:FLAG:GFP in pollen. We also crossed this transgenic plant expressing PiSSK1:FLAG:GFP with another previously generated transgenic S_2S_3 plant carrying the *LAT52*$_{pro}$:Myc:PiCUL1-P transgene (Li et al., 2016; Supplemental Figure S1A) to generate double transgenic plants expressing both PiSSK1:FLAG:GFP and Myc:PiCUL1-P in pollen. To circumvent SI, all pollinations were performed on pistils of immature flower buds, which produce a very low level of S-RNase that is insufficient to reject self-pollen (Ai et al., 1990; Sun and Kao, 2013). We then used pollen extracts of these two lines of double transgenic plants for Co-IP using a GFP-Trap agarose gel. We also used anti-Myc and anti-FLAG antibodies for immunoblotting to determine whether PiSSK1:FLAG:GFP co-immunoprecipitated with Myc:PiCUL1-P and Myc:PiCUL1-B. As controls, we also used pollen extracts from the transgenic plants expressing Myc:PiCUL1-B, Myc:PiCUL1-P, or PiSSK1:FLAG:GFP alone for Co-IP. As shown in Figure 1A, a protein of ~85-kDa, the size of Myc:PiCUL1-B, was detected only in the presence of PiSSK1:FLAG:GFP. Similarly, a ~85-kDa protein (Myc:PiCUL1-P) was detected only in the presence of PiSSK1:FLAG:GFP. Thus, both Myc:PiCUL1-P and Myc:PiCUL1-B co-immunoprecipitated with PiSSK1:FLAG:GFP in pollen protein extracts.

We next attempted to reconstitute the SCF^{SLF} complex in vitro using either PiCUL1-P or PiCUL1-B as the CUL1 subunit. We first separately co-expressed His-tagged PiCUL1-P or PiCUL1-B with GST-tagged S_2-SLF1 (Supplemental Figure S1C), and untagged PiSSK1 and PiRBX1, in High Five™ (Hi5) insect cells. We then used glutathione agarose to purify GST:S_2-SLF1 and its associated proteins in the co-expressed protein mixtures. As shown in Figure 1B, left side, a protein band of the expected size for GST:S_2-SLF1 (~70 kDa) was detected along with the band for either His:PiCUL1-P (~89 kDa) or His:PiCUL1-B (~89 kDa). The expected size of PiSSK1 is similar to that of GST, and thus they could not be separated on the gel, showing up as a band representing a mixture of these two proteins (labeled as PiSSK1 + GST Mix in Figure 1B). The PiRBX1 band was too weak to be detected in this experiment, so we also attempted to purify not only His:PiCUL1-B-associated proteins in the co-expressed mixture of His:PiCUL1-B, GST:S_2-SLF1, PiSSK1, and PiRBX1, but also His:PiCUL1-P-associated proteins in the co-expressed mixture of His:PiCUL1-P and PiRBX1, using HisPur™ Ni-NTA superflow agarose. In both experiments (Figure 1B, right side), we observed not only the purified band for either His:PiCUL1-B or His:PiCUL1-P, but also bands of the expected size for PiRBX1. These results, along with our in vivo experiments, suggest that both PiCUL1-P and PiCUL1-B can associate with SLF, PiSSK1, and PiRBX1 to form SCF^{SLF} complexes.

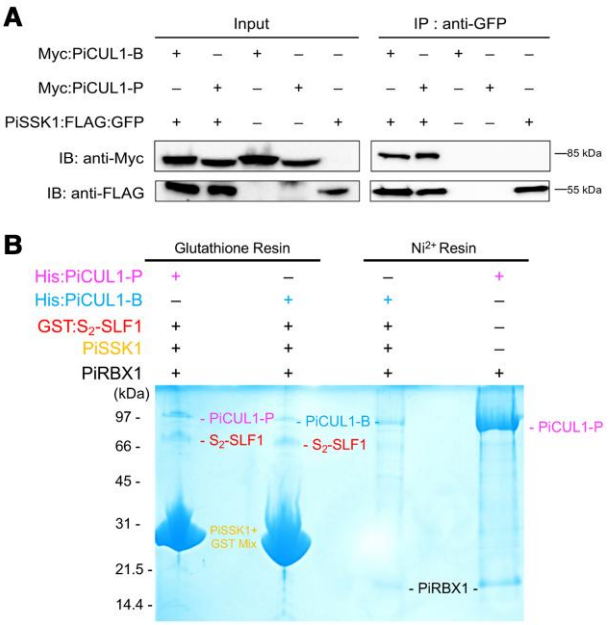

Figure 1 Both PiCUL1-P and PiCUL1-B of *Pe. inflata* can serve as Cullin1 subunits of SCF^{SLF} complexes. A, Co-immunoprecipitation of Myc:PiCUL1-P and Myc:PiCUL1-B with PiSSK1:FLAG:GFP. Total proteins were extracted from pollen collected from mature flowers of two lines of double transgenic plants each carrying *LAT52*$_{pro}$*:Myc:PiCUL1-P* and *LAT52*$_{pro}$*:PiSSK1:FLAG:GFP*, or *LAT52*$_{pro}$*:Myc:PiCUL1-B* and *LAT52*$_{pro}$*:PiSSK1:FLAG:GFP*, and from three lines of single transgenic plants each carrying *LAT52*$_{pro}$*:Myc:PiCUL1-P*, *LAT52*$_{pro}$*:Myc:PiCUL1-B*, or *LAT52*$_{pro}$*:PiSSK1:FLAG:GFP*. Extracted proteins were either separated by SDS-polyacrylamide gel electrophoresis (PAGE) for protein gel blot analysis (Input) or incubated with anti-GFP agarose gel (IP: anti-GFP). Protein extracts (Input) and IP products were subject to immunoblot analyses (IB), using either an anti-Myc or an anti-FLAG primary antibody as described in Materials and methods. Molecular masses of each of the three tagged proteins, Myc:PiCUL1-P, PiSSK1:FLAG:GFP, and Myc:PiCUL1-B, are indicated to the right of each blot. B, In vitro reconstitution of PiCUL1-P-containing or PiCUL1-B-containing SCF$^{S2\text{-}SLF1}$ complexes in insect cell culture. 50 µL of Ni^{2+} resin or glutathione resin was used in each lane for batch purification of protein complexes from 10 plates of Hi5 monolayer cells. Purified protein complexes were resolved by SDS-PAGE, and the gels were stained by Coomassie Brilliant Blue. Numbers to the left of the gel image represent marker sizes.

Transcripts of both *PiCUL1-B* and *PiCUL1-P* are present in anthers of *Pe. inflata*

For *PiCUL1-P* and *PiCUL1-B* to function in pollen for the SI in *Pe. inflata*, the transcripts of both genes would be expected to be present in anthers. Previously, our laboratory showed that the *PiCUL1-P* transcript was detected in anthers, pollen, and in vitro germinated pollen tubes. It was most abundant in anthers, especially in Stage 2 and Stage 3 anthers, where the levels were >100-fold higher than that in the other tissues examined (Li et al., 2014). Stage 2 anthers are from flower buds 0.5 to 1.0 cm in length, which contain free microspores released from tetrads, and Stage 3 anthers are

from flower buds 1.0 to 1.5 cm in length, which contain uninucleate microspores after nuclear migration (Mu et al., 1994).

To compare the transcript levels of *PiCUL1-P* and *PiCUL1-B*, we performed reverse transcription-quantitative polymerase chain reaction (RT-qPCR) on cDNA synthesized from total RNA isolated from Stage 2 and Stage 3 anthers, mature pollen, leaves, and styles of wild-type *Pe. inflata* plants of S_2S_3 genotype (Figure 2). The transcript levels of *PiCUL1-B* in both Stage 2 and Stage 3 anthers were significantly lower than those of *PiCUL1-P*, with the level in Stage 3 anthers ~5% that of *PiCUL1-P*. For both *PiCUL1-P* and *PiCUL1-B*, their respective transcript levels in leaves and styles were not significantly different (Figure 2A). The *PiCUL1-B* transcript level in Stage 3 anthers was significantly higher than the levels in Stage 2 anthers, mature pollen and leaf, but it was not significantly different from that in styles (Figure 2B). In contrast, the transcript levels of *PiCUL1-P* in both Stage 2 and Stage 3 anthers were significantly higher than those in mature pollen, leaf, and style (Figure 2C). Thus, both *PiCUL1-P* and *PiCUL1-B* were expressed in developing pollen contained in anthers, albeit the *PiCUL1-P* transcript was the predominant one.

SI behavior of pollen is not affected by knocking out *PiCUL1-P* alone or *PiCUL1-B* alone

To examine the biological functions of *PiCUL1-P* and *PiCUL1-B* in SI, we used polycistronic tRNA-gRNA (PTG)-based CRISPR/Cas9 genome editing (Xie et al., 2015; Sun and Kao, 2018; Sun et al., 2018) to separately generate frameshift indel alleles of either *PiCUL1-P* or *PiCUL1-B* in different transgenic *Pe. inflata* plants, and then generate double knockout mutants of both *PiCUL1-P* and *PiCUL1-B* (Figure 3).

To knockout *PiCUL1-P*, we chose a 20-bp sequence in the first exon of *PiCUL1-P* (116–135 bp counting from its start codon), as the protospacer sequence, designated *PiCUL1-P-Protospacer* (*PPS*; Figure 3A, magenta letters), for guiding Cas9 to specifically cleave this sequence. Similarly, to knockout *PiCUL1-B*, we chose a 20-bp protospacer sequence in its first exon (103–122 bp from its start codon), named *PiCUL1-B-Protospacer* (*BPS*; Figure 3A, blue letters). The *PPS-PTG* and *BPS-PTG*-containing CRISPR/Cas9 Ti-plasmids, both in pKSE401 (Supplemental Figure S2A; Xing et al., 2014; Sun and Kao, 2018; Sun et al., 2018), were separately introduced into wild-type *Pe. inflata* plants of S_2S_3 genotype via *Agrobacterium*-mediated transformation.

For *PiCUL1-P*, we identified one T_0 plant (PPS-T_0) that carried two frameshift indel alleles of *PiCUL1-P*: a 7-bp deletion allele, denoted as *−7bp*; and a 1-bp insertion allele, denoted as *+1C* (Figure 3B). These two indel alleles would result in defective proteins of 50 and 40 amino acid residues, respectively, if their transcripts were translated and the truncated proteins were not degraded (the full-length PiCUL1-P has 741 amino acids). Because the sequence of *PiCUL1-B* in the region corresponding to *PPS* differs from the *PPS* sequence by three nucleotides (Figure 3A, yellow shading), *PiCUL1-B* was not expected to be edited by CRISPR/Cas9 in PPS-T_0. We confirmed that the sequence of *PiCUL1-B* remained unaltered in PPS-T_0 by sequencing PCR fragments amplified from genomic DNA of PPS-T_0 using primers specific to *PiCUL1-B*. Primers used in this study are listed in Supplemental Table S2.

For *PiCUL1-B*, we identified one T_0 plant (BPS-T_0) that carried both a 1-bp deletion allele of *PiCUL1-B*, denoted as *−1C*, and an 8-bp deletion allele, denoted as *−8 bp* (Figure 3B). Similarly, the corresponding region of *BPS* in *PiCUL1-P* differs from *BPS* by two nucleotides (Figure 3A), thus the sequence of *PiCUL1-P* in the region corresponding to *BPS* was not altered in BPS-T_0, as confirmed by sequencing PCR fragments amplified from genomic DNA of BPS-T_0 using primers specific to *PiCUL1-P*.

To exclude both the possibility that genome editing was incomplete in the T_0 generation and the possible influence of the $35S_{pro}$:*Cas9* transgene, we used pollen from PPS-T_0 and BPS-T_0 to self-pollinate their own pistils in immature flower buds (known as bud-selfing), and identified bud-selfed progeny plants of PPS-T_0 and BPS-T_0 that lacked the $35S_{pro}$:*Cas9* transgene (Supplemental Figure S2B). In the bud-selfed progeny of PPS-T_0, we found three progeny plants that lacked the $35S_{pro}$:*Cas9* transgene: PBS-2 was homozygous for the *+1C* allele of *PiCUL1-P*; PBS-5 carried both the *+1C* allele and the *−7bp* allele; and PBS-6 was homozygous for the *−7bp* allele (Supplemental Figure S2C). We chose PBS-2 and PBS-6 to study their SI behavior, as both were homozygous for one of the indel alleles of *PiCUL1-P*, allowing us to examine the effect of each allele independent of the other. In the bud-selfed progeny of BPS-T_0, among the three progeny plants free of the $35S_{pro}$:*Cas9* transgene, BBS-2 carried both the *−8 bp* allele and the *−1C* allele of *PiCUL1-B*, BBS-4 was homozygous for the *−8 bp* allele, and BBS-5 was homozygous for the *−1C* allele (Supplemental Figure S2D). We chose BBS-4 and BBS-5 to study their SI behavior for the same reason that we had chosen PBS-2 and PBS-6. We further identified PBS-2 and BBS-4 as S_2S_3, and PBS-6 and BBS-5 as S_2S_2 (Supplemental Figure S2E). The genotypes of all of these single mutants of *PiCUL1-P* or *PiCUL1-B* are summarized in Supplemental Table S3.

To examine the SI behavior of these single mutants of *PiCUL1-P* or *PiCUL1-B*, we used their pollen to pollinate normally compatible wild-type pistils of S_3S_3, S_7S_7, and $S_{6a}S_{12}$ genotypes. If either PiCUL1-P or PiCUL1-B were essential for cross-compatible pollination, then both S_2 and S_3 pollen produced by the corresponding single mutant would be expected to be rejected by these normally compatible pistils. However, we found that all pollinations using pollen from either *PiCUL1-P* single mutants (PPS-T_0 and bud-selfed progeny plants PBS-2 and PBS-6) or *PiCUL1-B* single mutants (BPS-T_0 and bud-selfed progeny plants BBS-4 and BBS-5) remained compatible, with large size fruits obtained from each pollination (Figure 3C). Moreover, by aniline blue staining of pollen tube growth in the style, we observed that in each pollination, a large number of pollen tubes reached the bottom

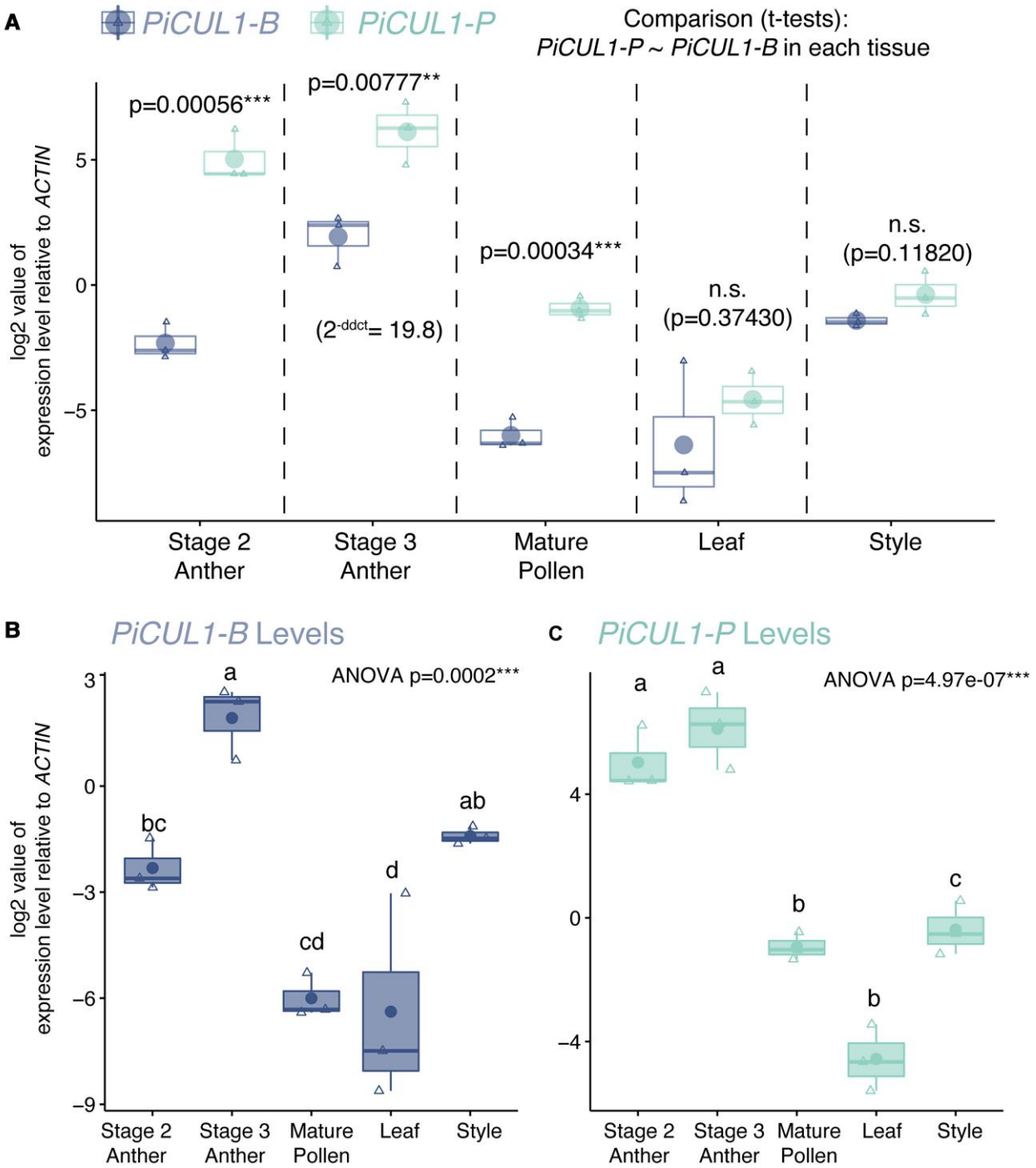

Figure 2 Transcript levels of *PiCUL1-B* and *PiCUL1*-P of *Pe. inflata* in various tissues and mature pollen. Transcript levels were determined using RT-qPCR as described in Materials and methods. A, Transcript levels of *PiCUL1-B* and *PiCUL1-P* in Stage 2 and Stage 3 anther, mature pollen, leaf, and style of wild-type *Pe. inflata* plants of the S_2S_3 genotype. B, Transcript levels of *PiCUL1-B* in Stage 2 and Stage 3 anther, mature pollen, leaf, and style of wild-type *Pe. inflata* plants of the S_2S_3 genotype. C, Transcript levels of *PiCUL1-P* in Stage 2 and Stage 3 anther, mature pollen, leaf, and style of wild-type *Pe. inflata* plants of the S_2S_3 genotype. Transcript levels of both *PiCUL1-B* and *PiCUL1-P* were normalized to *Pe. inflata ACTIN*. For each tissue and mature pollen, three biological replicates (from three independent wild-type plants) were examined, and each analysis used three technical replicates. For each tissue and mature pollen, the log2 value of the expression level of each gene relative to *ACTIN* was plotted in the box plot, with the upper and lower limits of each box showing 75th percentile and 25th percentile of the data, respectively, and the center horizontal line indicating the median value. The vertical line through each box indicates the range of the values (from minimum to maximum). The mean value of the three biological replicates for each gene in each tissue and mature pollen is shown in a circle in each box. For each gene, each individual data point in each biological replicate is shown in a triangle in the box plot. In (A), for each tissue and mature pollen, a *t* test was performed between

(continued)

segment of the style (Figure 3D). These results suggest that, in the presence of either PiCUL1-P alone or PiCUL1-B alone, pollen can still be accepted by pistils expressing nonself S-RNase. Therefore, neither PiCUL1-P nor PiCUL1-B is essential for cross-compatible pollination in *Pe. inflata*.

The SI behavior of *PiCUL1-P* and *PiCUL1-B* double knockout plants reveals their functional redundancy

These results led us to hypothesize that PiCUL1-P and PiCUL1-B function redundantly in cross-compatibility in *Pe. inflata*. To test this hypothesis, we generated double knockout mutants of both *PiCUL1-P* and *PiCUL1-B*. To this end, we used pollen from BPS-T_0 (S_2S_3 genotype) to pollinate PBS-6 (S_2S_2 genotype). These two plants were selected for two reasons: they were cross-compatible, yielding progeny with only the S_2S_3 genotype; and BPS-T_0 carried two deletion alleles of *PiCUL1-B* but was homozygous for wild-type *PiCUL1-P*, and PBS-6 was homozygous for the *−7bp* allele of *PiCUL1-P* but was homozygous for wild-type *PiCUL1-B*, and was free of the $35S_{pro}$:*Cas9* transgene (Supplemental Figure S2 and Table S3). This allowed us to obtain *Cas9*-free progeny that carried one copy of the *−7bp* allele of *PiCUL1-P* and one copy of wild-type *PiCUL1-P*, plus one copy of the *−1C* allele of *PiCUL1-B* and one copy of wild-type *PiCUL1-B* (Supplemental Figure S3A). We used one such progeny plant, which we named pxb, for bud-selfing to obtain three progeny plants. These were designated pxb-BS-A, pxb-BS-B, and pxb-BS-C, and were homozygous for both the *−7bp* allele of *PiCUL1-P* and the *−1C* allele of *PiCUL1-B* (Supplemental Figure S3A and Table S3). As a result, these three plants did not produce any functional PiCUL1-P or PiCUL1-B. The S-genotypes of pxb-BS-A, pxb-BS-B, and pxb-BS-C were S_2S_2, S_2S_3, and S_3S_3, respectively (Supplemental Figure S3B and Table S3), and all were confirmed to be free of the $35S_{pro}$:*Cas9* transgene (Supplemental Figure S3C and Table S3).

To examine the effect of the double knockout of *PiCUL1-P* and *PiCUL1-B* on pollen SI behavior, we used pollen from pxb-BS-A (S_2S_2) and pxb-BS-B (S_2S_3) to pollinate S_3S_3, S_7S_7, and $S_{6a}S_{12}$ pistils, and we used pollen from pxb-BS-C (S_3S_3) to pollinate S_7S_7 and $S_{6a}S_{12}$ pistils. All these pollinations would normally be compatible; however, all were incompatible, with no fruit set (Figure 3C). Aniline blue staining of pollen tubes in the style pollinated by pollen from these double mutants of *PiCUL1-P* and *PiCUL1-B* also showed that the growth of most pollen tubes stopped in the top part of the style, with no pollen tubes found at the bottom of the style (representative results of pxb-BS-A are shown in Figure 3D). This is characteristic of the growth arrest of incompatible pollen tubes.

To examine whether rejection of pollen was due to S-RNase activity, we used pollen from pxb-BS-A and pxb-BS-B to pollinate an S_3S_3 transgenic plant (denoted *As-*S_3/S_3S_3), in which production of S_3-RNase was suppressed by an antisense S_3-*RNase* transgene (Lee et al., 1994; Sun and Kao, 2013, 2018; Sun et al., 2018). All these pollinations were completely compatible, setting large size fruits (Figure 3, C and D), suggesting that, as long as a pistil does not produce any nonself S-RNase, pollen can be accepted and effect fertilization even in the absence of both PiCUL1-P and PiCUL1-B.

Based on all these results, we can make three conclusions: that either PiCUL1-P alone or PiCUL1-B alone is sufficient for SLF proteins to function in the context of SCF^{SLF} complexes to detoxify nonself S-RNases to allow cross-compatible pollination; that in the absence of both PiCUL1-P and PiCUL1-B, no other CUL1 proteins produced in pollen (PiCUL1-C, PiCUL1-G, and PiCUL1-E) can substitute for them in inhibiting nonself S-RNase during pollination; and that both PiCUL1-P and PiCUL1-B function specifically in cross-compatibility.

As our results showed that PiCUL1-P and PiCUL1-B function redundantly in cross-compatibility in pollen and that the level of the *PiCUL1-P* transcript was higher than that of *PiCUL1-B* in pollen (Figure 2A), we further hypothesized that when functional PiCUL1-P is absent in pollen, the transcript level of functional *PiCUL1-B* might be elevated to compensate for the loss of PiCUL1-P to ensure complete inhibition of nonself S-RNases by pollen. To test this hypothesis, we examined the transcript level of *PiCUL1-B* in Stage 2 and Stage 3 anthers of bud-selfed progeny of PBS-6 (denoted PBS-6-BS in Supplemental Figure S4), a *Cas9*-free S_2S_2 plant homozygous for the *−7bp* allele of *PiCUL1-P* and wild-type allele of *PiCUL1-B* (Supplemental Figure S2 and Table S3). However, contrary to this hypothesis, we did not find any significant change in the transcript level of *PiCUL1-B* in either Stage 2 or Stage 3 anthers of these *PiCUL1-P* single knockout mutant plants (Supplemental Figure S4). Even though the transcript level of *PiCUL1-B* was not elevated in the absence of functional PiCUL1-P in PBS-6-BS plants, all of these *PiCUL1-P* single knockout mutants were compatible with S_3S_3 and $S_{6a}S_{12}$ pistils. These results also suggest that the transcript level of *PiCUL1-B* alone, albeit lower than that of *PiCUL1-P* (Figure 2A), is sufficient for the production of the CUL1 subunit required for the assembly of functional SCF^{SLF} complexes to mediate degradation of nonself S-RNases.

CUL1-P and CUL1-B interact specifically with SSK1 in SCF^{SLF} complexes in *Pe. inflata*

In addition to *PiCUL1-P* and *PiCUL1-B*, the *Pe. inflata* genome contains three genes encoding CUL1 proteins: PiCUL1-C, PiCUL1-G, and PiCUL1-E, all of which are expressed in pollen

Figure 2 (Continued)
the mean values for *PiCUL1-P* and *PiCUL1-B*, and the resulting *P*-value of each *t* test is shown above each pair of boxes. In (B) and (C), a one-way analysis of variance was performed among the mean values for *PiCUL1-B*, and pairwise ad-hoc Tukey's tests were then performed among the mean values, with different letters above each box indicating statistically significant differences. ***$P \leq 0.001$; **$P \leq 0.001$; n.s., not significant, with $P > 0.05$. The results of all the statistical tests are shown in Supplemental Data Set 2A–C.

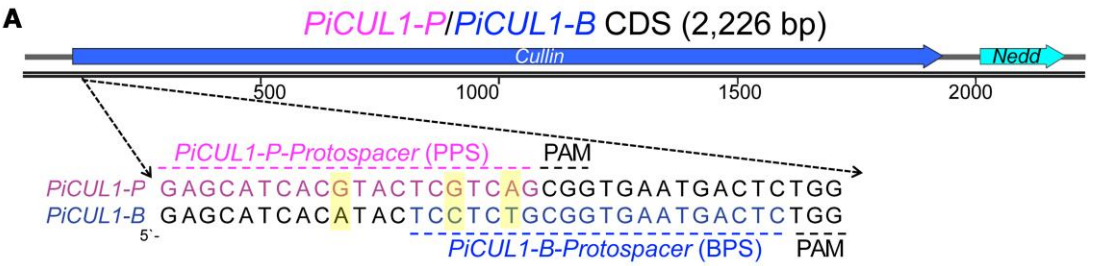

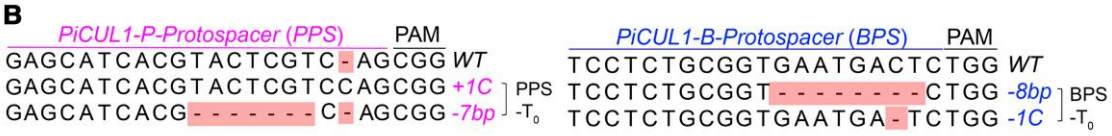

C

	♂			♀			
Plant	*PiCUL1-P*	*PiCUL1-B*	*S*	S_7S_7	$S_{6a}S_{12}$	S_3S_3	*As-*S_3 /S_3S_3
PPS-T_0	*-7bp/+1C*	*WT/WT*	S_2S_3	+	+	+	N.D.
PBS-2	*+1C/+1C*		S_2S_3	+	+	+	N.D.
PBS-6	*-7bp/-7bp*		S_2S_2	+	+	+	N.D.
BPS-T_0	*WT/WT*	*-8bp/-1C*	S_2S_3	+	+	+	N.D.
BBS-4		*-8bp/-8bp*	S_2S_3	+	+	+	N.D.
BBS-5		*-1C/-1C*	S_2S_2	+	+	+	N.D.
pxb-BS-A	*-7bp/-7bp*	*-1C/-1C*	S_2S_2	–	–	–	+
pxb-BS-B			S_2S_3	–	–	–	+
pxb-BS-C			S_3S_3	–	–	N.D.	N.D.

D

	♂			♀			
Plant	*PiCUL1* -P	*PiCUL1* -B	*S*	S_3S_3	*As-*S_3/S_3S_3	S_7S_7	$S_{6a}S_{12}$
PBS-6	*-7bp/-7bp*	*WT/WT*	S_2S_2		N.D.		
BBS-5	*WT/WT*	*-1C/-1C*	S_2S_2		N.D.		
pxb-BS-A	*-7bp/-7bp*	*-1C/-1C*	S_2S_2				

Figure 3 CRISPR/Cas9-mediated knockout of PiCUL1-P and PiCUL1-B, and the self-incompatibility behavior of knockout plants. A, The protospacers specifically targeting *PiCUL1-P* and *PiCUL1-B*. Coding sequences of either *PiCUL1-P* or *PiCUL1-B* predicted to encode the Cullin domain (Pfam: 00888) and the Neddylation (*Nedd*) domain (Pfam: 10557) are indicated in two arrows. A 20-bp sequence (named *PiCUL1-P-Protospacer*, *PPS*) of the antisense strand of *PiCUL1-P*, followed by the PAM motif (CGG), was chosen as the protospacer for CRISPR/Cas9. There are three mismatches (highlighted nucleotides) in the corresponding 20-bp region in *PiCUL1-B*. A 20-bp sequence (named *PiCUL1-B-Protospacer*, *BPS*) of the antisense strand of *PiCUL1-B*, followed by the PAM motif (TGG), was chosen as the protospacer for CRISPR/Cas9. Two of the three mismatches (highlighted nucleotides) are found in the corresponding 20-bp region in *PiCUL1-P*. B, Sequences of frameshift indel alleles of *PiCUL1-P* (left) or *PiCUL1-B* (right) generated using CRISPR/Cas9 in T_0 plants. For *PiCUL1-P*, in the T_0 plant PPS-T_0, a 7-bp deletion allele, denoted *−7bp* and a 1-bp insertion allele, denoted *+1C* in the edited region of *PiCUL1-P* were generated. For *PiCUL1-B*, in the T_0 plant BPS-T_0, a 1-bp deletion allele denoted *−1C* and an 8-bp deletion allele denoted *−8 bp* in the edited region of *PiCUL1-B* were generated. The sequences shown are those of the antisense strand of *PiCUL1-P* and *PiCUL1-B* (5′ to 3′ from left to right). C, Results of pollination using pollen from *PiCUL1-P* knockout plants,

(continued)

(Hua and Kao, 2006). Their orthologs in *Pe. hybrida* are also expressed in pollen (Kubo et al., 2016). In addition to the pollen-specific *PiSSK1*, the *Pe. inflata* genome contains 16 genes encoding Skp1 proteins, and the transcripts of nine of them were found in the pollen transcriptomes of the S_2-haplotype and/or S_3-haplotype (Sun and Kao, 2018). Our biochemical and genetic results suggest both that none of these nine Skp1 proteins can interact with PiCUL1-P or PiCUL1-B, and that none of the other three CUL1 proteins can interact with PiSSK1 to form SCF^{SLF} complexes in pollen. To identify the amino acid residues of PiCUL1-P and PiCUL1-B involved in their specific interaction with PiSSK1, we first performed protein modeling of the SCF^{SLF} complex containing PiSSK1, PiCUL1-P or PiCUL1-B, PiRBX1, and S_2-SLF1 (Supplemental Figure S5A), using AlphaFold2 (Mirdita et al., 2022). We then investigated the amino acid residues predicted to be at the interface between PiSSK1 and either PiCUL1-P, or PiCUL1-B, in these predicted protein complex models (Supplemental Figure S5B). At the PiCUL1-P/PiCUL1-B and PiSSK1 interface, six amino acids were found to be unique to PiCUL1-P and PiCUL1-B, but divergent in the other three CUL1 proteins (Supplemental Figure S5C). Therefore, these six amino acids are good candidates for the amino acid residues that are involved in the specific interactions of PiSSK1 with PiCUL1-P and PiCUL1-B.

Petunia hybrida PhCUL1-B also is capable of serving as the CUL1 subunit of SCF^{SLF} complexes

The results described so far provided strong evidence that, in *Pe. inflata*, both PiCUL1-P and PiCUL1-B can serve as the CUL1 subunit of SCF^{SLF} complexes to allow pollen to inhibit nonself S-RNases. However, in a previous study of the function of CUL1-P in SI, Kubo et al. (2016) used amiRNA to knockdown the expression of *CUL1-P* in *Pe. hybrida* plants. They found that pollen that had the production of PhCUL1-P significantly repressed by amiRNA showed reduced fertility when it was used to pollinate pistils of nonself S-genotypes. This suggested both that PhCUL1-P is essential for pollen function during compatible pollination in *Pe. hybrida*, and that in the absence of PhCUL1-P, PhCUL1-B could not substitute for PhCUL1-P. The different roles of PiCUL1-B and PhCUL1-B was puzzling, especially considering that PhCUL1-B and PiCUL1-B share 97.8% sequence identity in their deduced amino acid sequences. Moreover, the Skp1 adaptor subunit in both species, PhSSK1 and PiSSK1, differ only in two adjacent amino acid residues in the middle of the protein (S78 and E79 in PiSSK1, and G78 and K79 in PhSSK1; Supplemental Figure S1B). In addition, all the six amino acids at the predicted interface with PiSSK1 in SCF^{SLF} complexes in *Pe. inflata* are shared by PhCUL1-P and PhCUL1-B, but they are divergent in the other *Pe. hybrida* CUL1 proteins (highlighted in yellow with red asterisks in Supplemental Figure S5C).

To resolve the contradictory results regarding the role of PhCUL1-B, we first examined whether PhCUL1-B could interact with PiSSK1 and PhSSK1 in vivo (Figure 4A). To this end, we made transgene constructs $LAT52_{pro}$:*Myc:PhCUL1-B* (Supplemental Figure S1A) and $LAT52_{pro}$:*PhSSK1:FLAG:GFP* (Supplemental Figure S1B), and used them to separately transform *Pe. inflata* plants of S_2S_3 genotype. We then chose one plant from each transgenic line that expressed high levels of the corresponding tagged protein, and crossed them to obtain double transgenic plants co-expressing Myc:PhCUL1-B and PhSSK1:FLAG:GFP. We also crossed the transgenic plant expressing Myc:PhCUL1-B with a transgenic plant expressing PiSSK1:FLAG:GFP (Supplemental Figure S1B) to generate double transgenic plants co-expressing Myc:PhCUL1-B and PiSSK1:FLAG:GFP. All pollinations were performed using flower buds to circumvent SI. Protein extracts from pollen of these three lines of double transgenic plants, and from pollen of the double transgenic plant described earlier that co-expressed Myc:PiCUL1-B and PiSSK1:FLAG:GFP, were analyzed by IP using a GFP-Trap agarose gel. An anti-Myc antibody was used for protein blotting to determine whether PiSSK1:FLAG:GFP and PhSSK1:FLAG:GFP co-immunoprecipitated with Myc:PiCUL1-B and Myc:PhCUL1-B. Consistent with the results shown in Figure 1A, Myc:PiCUL1-B co-immunoprecipitated with PiSSK1:FLAG:GFP, and it also co-immunoprecipitated with PhSSK1:FLAG:GFP (Figure 4A). Interestingly, we found that Myc:PhCUL1-B also co-immunoprecipitated with both PhSSK1:FLAG:GFP and PiSSK1:FLAG:GFP (Figure 4A). These results suggest that, like PiCUL1-B, PhCUL1-B can interact with both PhSSK1 and PiSSK1 in vivo.

The Co-IP results also suggest that, when expressed to a high level in pollen (driven by the strong pollen-specific *LAT52* promoter), PhCUL1-B can serve as the CUL1 subunit

Figure 3 (Continued)
PiCUL1-B knockout plants, and double knockout plants of both *PiCUL1-P* and *PiCUL1-B*, to separately pollinate pistils of various *S*-genotypes. The *S*-genotypes of the knockout plants used as male parents (♂) are shown under the column labeled "S," and the *S*-genotypes of three wild-type plants used as female parents (♀) are indicated. *As-*S_3/S_3S_3: a transgenic plant that did not produce any S_3-RNase due to suppression of its expression by an antisense S_3-*RNase* gene. Each pollination was repeated at least three times with reproducible outcomes. "−" indicates incompatible pollination with no fruit set; "+" indicates compatible pollination with large fruits. D, Representative aniline blue staining images of pollen tubes in the bottom segment of the style of wild-type S_3S_3, S_7S_7, and $S_{6a}S_{12}$ plants, and transgenic plant *As-*S_3/S_3S_3, pollinated by a *PiCUL1-P* knockout plant (PBS-6), a *PiCUL1-B* knockout plant (BBS-5), and a double knockout plants of both *PiCUL1-P* and *PiCUL1-B* (pxb-BS-A). The *S*-genotypes of these three representative knockout plants used as male parents (♂) are shown under the column labeled *S*, and the *S*-genotypes of three wild-type plants and *As-*S_3/S_3S_3 used as female parents (♀) are indicated. The presence of a large number of pollen tubes in this segment of the style indicates compatible pollination. In the case of incompatible pollinations, very few pollen tubes (indicated by arrows) can be observed in this segment of the style. N.D., not determined. Scale bar = 0.25 mm.

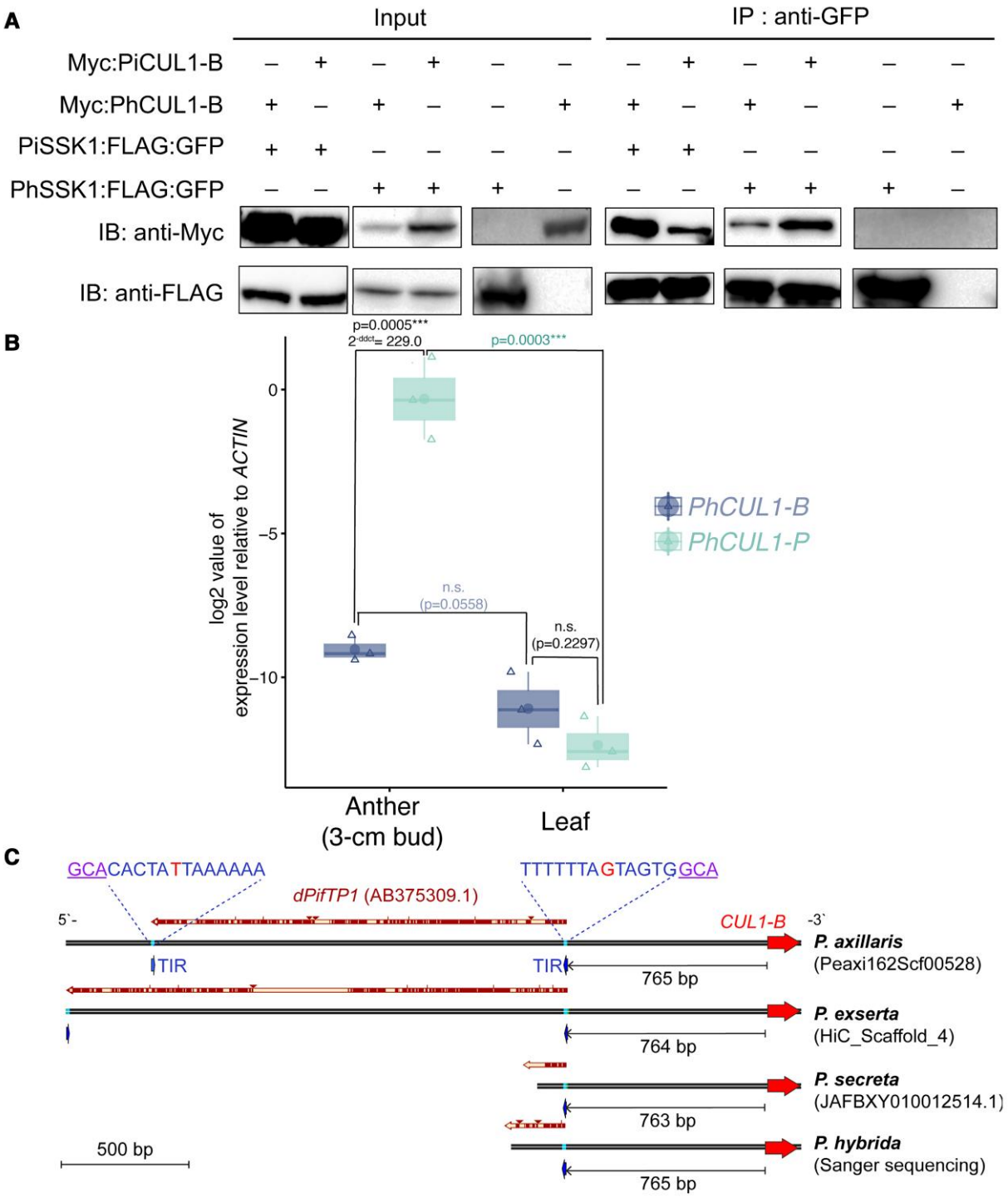

Figure 4 *Petunia hybrida* PhCUL1-B can serve as a CUL1 subunit of SCF^{SLF} complexes, but its transcript level is drastically reduced. A, Co-immunoprecipitation of Myc:PiCUL1-B and Myc:PhCUL1-B by either PhSSK1:FLAG:GFP or PiSSK1:FLAG:GFP. Total proteins were extracted from pollen collected from mature flowers of five lines of transgenic plants, each carrying *LAT52$_{pro}$:Myc:PhCUL1-B* and *LAT52$_{pro}$:PiSSK1:FLAG:GFP*, *LAT52$_{pro}$:Myc:PhCUL1-B* and *LAT52$_{pro}$:PhSSK1:FLAG:GFP*, *LAT52$_{pro}$:Myc:PiCUL1-B* and *LAT52$_{pro}$:PiSSK1:FLAG:GFP*, *LAT52$_{pro}$:Myc:PhCUL1-B*, or *LAT52$_{pro}$:PhSSK1:FLAG:GFP*. To assess interactions of Myc:PhCUL1-B with PiSSK1:FLAG:GFP and PhSSK1:FLAG:GFP by co-immunoprecipitation, the protein extracts were either separated by SDS-PAGE for protein gel blot analysis (Input), or incubated with anti-GFP agarose gel (IP: anti-GFP), as described in the legend to Figure 1A. B, Transcript levels of *PhCUL1-P* and *PhCUL1-B* in anther and leaf of *P. hybrida*, as assessed by RT-qPCR. Anthers were collected from flower buds 3 cm in length. Transcript levels were normalized to the *Petunia ACTIN*. For each tissue, three biological replicates (from three *Pe. hybrida* plants) were examined, and each contained three technical replicates. For each tissue, the log2 value of the expression level of each gene relative to the *Petunia ACTIN* was plotted in the box plot, and the other elements in the box plots are defined as described in the legend to Figure 2. Results of *t* tests between the mean values for *PhCUL1-P* and *PhCUL1-B* are shown above the connecting

(continued)

in SCF^{SLF} complexes. We therefore suspected that the difference in the SI phenotype of the amiRNA-mediated knockdown mutant of *PhCUL1-P* reported by Kubo et al. (2016) and our CRISPR/Cas9-mediated knockout of *PiCUL1-P* might be due to the difference in the abundance of *CUL1-B* in *Pe. inflata* and *Pe. hybrida*. Indeed, in *Pe. hybrida*, the transcript level of *PhCUL1-P* was most abundant in anthers, reaching its peak in anthers from flower buds that were 3 cm in size, while the transcript of *PhCUL1-B* was reported to be present at very low levels in all the tissues examined (Kubo et al., 2016). Consistent with this observation by Kubo et al. (2016), when we examined the transcript levels of *PhCUL1-P* and *PhCUL1-B* in anthers from 3-cm flower buds and in leaves of the *Pe. hybrida* plants used in this study, we found that the transcript level of *PhCUL1-P* was over 200-fold higher than that of *PhCUL1-B* in 3-cm anthers, and the transcript level of *PhCUL1-B* was similarly low in anthers and leaves (Figure 4B). Thus, the loss of PhCUL1-B function observed by Kubo et al. (2016) was likely caused by low transcript levels of *PhCUL1-B* in pollen rather than by the inability of PhCUL1-B to function as the CUL1 subunit of SCF^{SLF} complexes.

A DNA transposon is potentially responsible for the reduced transcript level of *CUL1-B* in *Pe. hybrida*

Why is there a drastic reduction in the transcript level of *PhCUL1-B* in anthers? To answer this, we first compared the promoter region of *CUL1-B* in the genome sequences of *Pe. inflata* and a self-compatible S_N genotype of *Pe. axillaris* (Bombarely et al., 2016) because *Pe. inflata* and *Pe. axillaris* were two parental species used in the creation of *Pe. hybrida*. (All genome databases used in this work are listed in Supplemental Table S4.) Notably, in a genomic region ~750 bp to ~2.3 kb upstream from the start of the first exon of *CUL1-B* of *Pe. axillaris* (*PaCUL1-B*), we found sequences resembling the sequence of a *Petunia* inhibitor/defective *spm*-like transposable element named *dPifTp1* (Matsubara et al., 2008; Figure S4C). This region contained two 13-bp terminal inverted repeats (TIRs) with only one mismatch, which were flanked by two target-site duplication (TSD) sequences of 5′-GCA-3′ (underlined in Figure 4C). This *dPifTp1*-like sequence was not found in the corresponding genomic region upstream from *PiCUL1-B* in the *Pe. inflata* genome, as the upstream flanking regions of *PiCUL1-B* and *PaCUL1-B* showed little sequence similarity (Supplemental Figure S6A). We then used PCR to amplify a ~1-kb genomic sequence of the *Pe. hybrida* plant we used in this study, upstream from the start codon of *PhCUL1-B*. Interestingly, we found this sequence to share a very high degree of sequence similarity with the corresponding upstream sequence of *PaCUL1-B*, including one of the TIR regions mentioned above (Figure 4C). The insertion of *dPifTp1* in the second intron of *Floral Binding Protein 2* (*FBP2*) was shown to result in a drastic reduction in the transcript level of *FBP2* in a *Pe. inflata Green Corolla Segment* mutant (Matsubara et al., 2008). Therefore, the very low transcript level of *PhCUL1-B* (Figure 4B; Kubo et al., 2016) could be due to the presence of the *dPifTp1*-like transposable element in the promoter region of *PhCUL1-B*, which was most likely inherited from *Pe. axillaris*.

In addition, in the genomes of two other *Petunia* species, *Petunia exserta*, and *Petunia secreta* (Berardi et al., 2021), we identified one *CUL1-P* gene and one *CUL1-B* gene (Supplemental Table S5). In both genomes, we also found *dPifTp1*-like sequences upstream from *CUL1-B* (Figure 4C). *Petunia axillaris*, *Pe. exserta*, and *Pe. secreta* belong to the long-tube clade of *Petunia*, while *Pe. inflata* belongs to the short-tube clade (Reck-Kortmann et al., 2014; Berardi et al., 2021). Thus, the *dPifTp1*-like TE insertion in the promoter region of *CUL1-B* might have occurred after the divergence of the long-tube and the short-tube clades in *Petunia*.

In contrast to the upstream regions of *CUL1-B*, the upstream sequences of *CUL1-P* in *Pe. inflata* (*PiCUL1-P*) and *Pe. axillaris* (*PaCUL1-P*) shared remarkable sequence similarity up to ~1.6 kb upstream (to the end of a *WD40* gene) of the *CUL1-P* genes (Supplemental Figure S6B). This finding could explain the similar pollen-specific expression profiles of *PiCUL1-P* and *PhCUL1-P* (Figures 2A and 4B; Li et al., 2014; Kubo et al., 2016).

CUL1-B is absent in the other Solanaceae species examined

From phylogenetic analysis of Solanaceae *CUL1* genes, Kubo et al. (2016) reported that *CUL1-B* was only found in *Petunia*, and that each of the other diploid Solanaceae species analyzed only possessed one gene in the same clade with *Petunia CUL1-P* (Kubo et al., 2016). In the draft genome of a self-incompatible wild tomato species, *Solanum chilense* (Stam et al., 2019), we also identified only one copy of the *CUL1-P* homolog, which showed ~91% sequence identity with *PiCUL1-P* (Supplemental Table S5). This suggested that the lack of a second *CUL1-P* homolog in the previously

Figure 4 (Continued)
lines for each pair compared. ***$P \leq 0.001$; n.s., not significant, with $P > 0.05$. The results of all the statistical tests are shown in Supplemental Data Set 2D. C, Schematic showing alignment of a *dPifTp1* DNA transposon sequence (2,123 bp) and the upstream regions of *CUL1-B* in three *Petunia* species in the long-tube clade (*Pe. axillaris*, *Pe. exserta*, and *Pe. secreta*) and *Pe. hybrida*. The sequence in each dark red region matches the *dPifTp1* sequence. Two TIRs are indicated in blue arrows, and the mismatches between the two TIR sequences are indicated in red. The TSD sequences are underlined. Because the *CUL1-B*-containing scaffold in the *Pe. secreta* genome only contains 763 bp of the upstream sequence of *CUL1-B*, only one TIR sequence is shown. Only one TIR sequence was contained in the Sanger sequencing result of the upstream region of *PhCUL1-B* we amplified.

analyzed Solanaceae species, except *Petunia*, is not associated with the lack of SI.

To better determine the presence or absence of *CUL1-P* and *CUL1-B* in the Solanaceae, we further examined syntenic relationships between the *CUL1-P*-containing scaffolds (or the *CUL1-B*-containing scaffolds) in three *Petunia* genomes and four other Solanaceae genomes, including tomato (Hosmani et al., 2019) and three *Nicotiana* species: diploid *Nicotiana attenuata* (Xu et al., 2017), diploid *Nicotiana tomentosiformis* (Sierro et al., 2013), and allotetraploid *Nicotiana benthamiana* (on two different genomic scaffolds; Bombarely et al., 2012; Figure 5). Syntenic analysis of the flanking genomic regions of *CUL1-P* orthologs revealed a syntenic block shared by *Petunia* and tomato, as well as by *Petunia* and three *Nicotiana* species (Figure 5A). In contrast, the scaffolds containing *CUL1-B* in the three *Petunia* genomes was found to be mostly syntenic with genomic regions on Chromosome 4 of tomato, which did not contain *CUL1*, but contained a gene encoding a PLN03218 superfamily protein that contains multiple pentatricopeptide repeat (PPR) motifs (Figure 5B). In the three *Nicotiana* genomes, the scaffolds syntenic with the *Petunia CUL1-B*-containing scaffolds also lacked any *CUL1*, but all contained the same *PLN03218* homologs (Figure 5B). These results further support that *CUL1-B* is absent in the crown-group clade of the Solanaceae, which contains both *Nicotiana* and *Solanum* (Olmstead et al., 2008; Särkinen et al., 2013; Bombarely et al., 2016), and its location has been replaced by the *PLN03218* superfamily gene.

Duplication mechanism of SI-specific *CUL1* genes in *Petunia*

To better understand the mechanism underlying the duplication event that gave rise to *CUL1-P* and *CUL1-B* in *Petunia*, we compared the flanking noncoding regions of these two genes in *Pe. inflata* and *Pe. axillaris*. The flanking regions of *CUL1-P* and *CUL1-B* in the *Pe. inflata* genome shared little sequence similarity (Supplemental Figure S7A). The flanking regions of *CUL1-P* and *CUL1-B* in the *Pe. axillaris* genome also shared little sequence similarity (Supplemental Figure S7B). Furthermore, in all the *Petunia* genomes we examined, *CUL1-P* and *CUL1-B* were found on different genomic scaffolds (Supplemental Tables S1 and Table S5), and they were flanked by different genes (Figure 5). Overall, our comparative analyses of the *Petunia* genomes suggest that the duplication event that gave rise to *CUL1-P* and *CUL1-B* is not likely simply a local (tandem or proximal) duplication or a segmental duplication of *CUL1-P*, but rather arose via dispersed duplication (Moore and Purugganan, 2003; Ganko et al., 2007; Wang et al., 2016; Qiao et al., 2019).

Possible origin of SI-specific *CUL1* genes in the Solanaceae

To better understand the evolution of the genes encoding the CUL1 subunit involved in S-RNase-based SI in the Solanaceae, we analyzed the phylogenetic relationship among all Cullin proteins encoded in the genomes of species in various eudicot families in both the Superasterid and Rosid groups (Figure 6; Supplemental Figure S8, Files 1 and 2). The phylogenetic relationship of these species analyzed is shown in Figure 6A, and the genomes analyzed are listed in Supplemental Table S4. Only Cullin proteins (including CUL1, CUL3, and CUL4) that contain both a complete Cullin domain and a complete Neddylation domain (Ban and Estelle, 2021) were included in this phylogenetic analysis.

The results of the phylogenetic analysis showed that the clade of CUL1-C was shared by both Asterids and Rosids, while a clade of Rosid CUL1s (here named CUL1-R) and a clade of Superasterid CUL1s (here named CUL1-SA) were found on a branch distinct from the CUL1-C clade (Figure 6B; Supplemental Figure S8). In the CUL1-SA clade, the Solanaceae contains three clades of CUL1, namely CUL1-P/CUL1-B, CUL1-E, and CUL1-G/CUL1-D (CUL1-D in other Solanaceae species is orthologous to *Petunia* CUL1-G; Kubo et al., 2016). Within the CUL1-SA clade, these three Solanaceae-specific clades are found in the same clade along with one CUL1 each from *Ipomoea tribola* (itb14g21010), *Antihinum majus* (Am01g40480), and *Coffea canephora* (Cc01t20500; Figure 6B). These results suggest that all three clades of Solanaceae-specific CUL1s share the same origin in the CUL1-SA clade in the Superasterids, which is a sister clade to the CUL1-R clade found in Rosids.

We further performed syntenic analyses among the *CUL1-SA*-containing scaffolds in the *Pe. inflata* genome, as well as between the *CUL1-SA*-containing scaffolds of *Pe. inflata* and genomic regions containing *CUL1-SA* genes in *I. tribola* and *Cof. canephora* (Figure 7). We found that the genome sequence scaffolds containing *PiCUL1-P*, *PiCUL1-E*, or *PiCUL1-G* shared gene synteny in the region flanking the three *CUL1* genes, especially between the *PiCUL1-P*-containing and *PiCUL1-E*-containing scaffolds (Figure 7A). These three scaffolds also shared synteny with genes flanking *itb14g21010*, the only *CUL1-SA* gene in the *I. tribola* genome, located on Chromosome 14 (Figure 7B). In the *Cof. canephora* genome, two genes, *zf-CW* (encoding a CW-type zinc-finger protein) and *PEX6* (encoding peroxisomal biogenesis factor 6) located downstream from the *CUL1-SA* gene, *Cc01t20500*, were syntenic with the corresponding genes downstream from *PiCUL1-P*, and the genes upstream from this *CUL1* gene of *Cof. canephora* were syntenic with the genes upstream from *PiCUL1-E* (Figure 7C). We also compared the gene synteny between the *PiCUL1-B*-containing scaffold of *Pe. inflata*, Peinf101Scf01172, and the genomes of *I. tribola*, *A. majus*, and *Cof. canephora*. In each of these genomes, at least one region syntenic with Peinf101Scf01172 was found, but none contained either *CUL1* or *PLN03218* (Supplemental Figure S9).

Taken together, our phylogenetic and syntenic analyses suggest that Solanaceae CUL1-P, CUL1-E, and CUL1-G/CUL1-D have likely been derived from a shared common ancestral *CUL1* in the *CUL1-SA* clade. As illustrated in Figure 8, the proliferation of the *CUL1-SA* clade genes in the Solanaceae might be a result of the Solanaceae-specific whole-genome triplication event (WGT; Bombarely et al.,

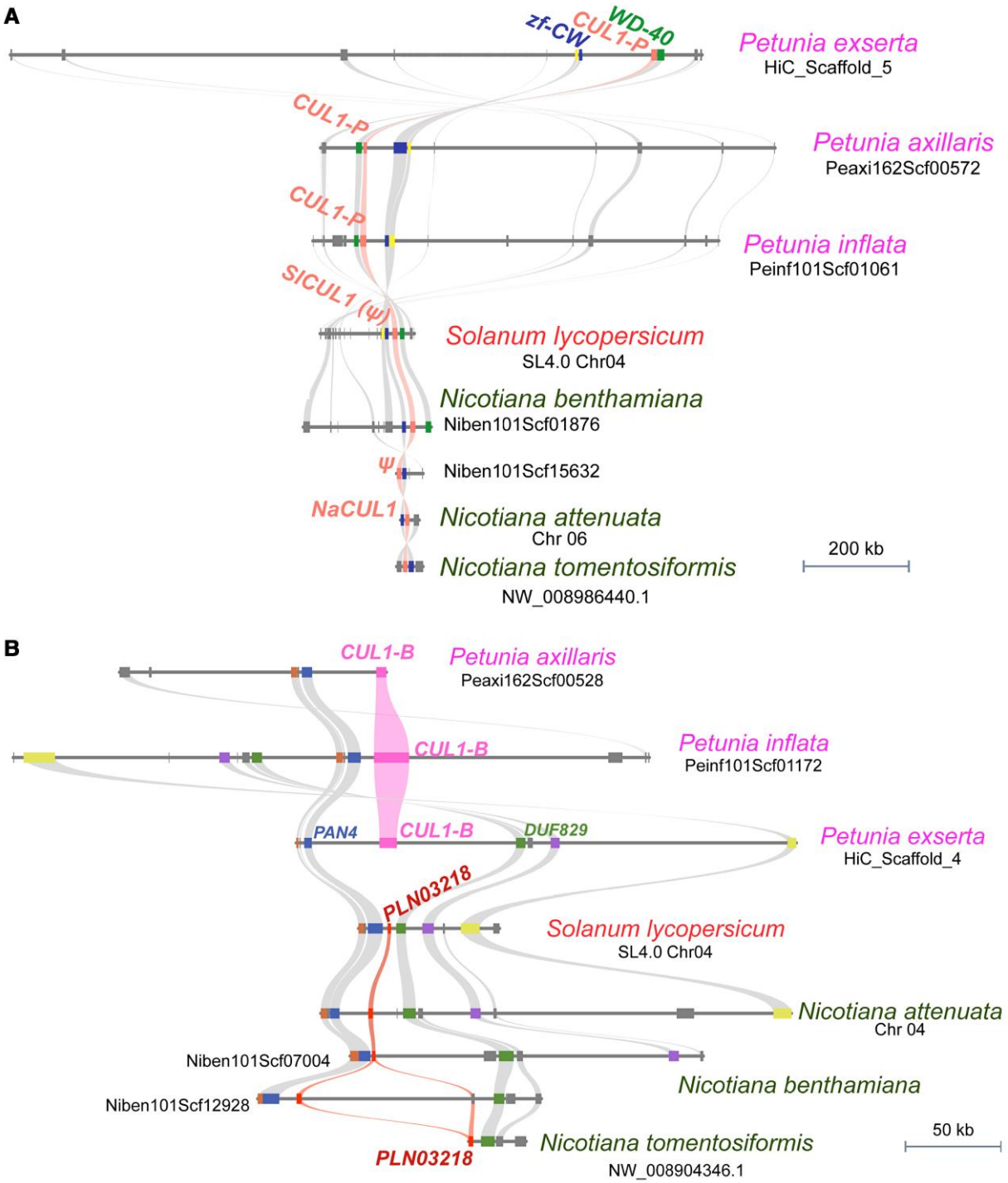

Figure 5 Syntenic relationships between the *CUL1-P*-containing scaffolds, or between the *CUL1-B*-containing scaffolds in three *Petunia* genomes, and four other Solanaceae genomes. The three *Petunia* species analyzed are *Pe. inflata*, *Pe. axillaris*, and *Pe. exserta*. The other Solanaceae species analyzed are tomato (*S. lycopersicum*) and three *Nicotiana* species: diploid *N. tomentosiformis* and *N. attenuata*, and allotetraploid *N. benthamiana*. Blocks of the same color indicate homologous genes. A, Syntenic relationship between the *CUL1-P*-containing scaffolds of *Petunia* and chromosomal regions of tomato and three *Nicotiana* genomes. Gene abbreviations: *WD40*, encoding a protein containing multiple WD40 motifs; *zf-CW*, encoding a CW-type zinc-finger protein. Both the *CUL1-P* ortholog in tomato (*SlCUL1*; *Solyc06g008710.3.1*) and one of the two *CUL1-P* orthologs in the *N. benthamiana* genome (on Niben101Scf15632) are pseudogenes and labeled with a ψ symbol. B, Syntenic relationship between the *CUL1-B*-containing scaffolds of *Petunia* and chromosomal regions of tomato and three *Nicotiana* genomes. Gene abbreviations: *DUF829*, encoding a protein of unknown function containing a DUF829 domain (Pfam: cl05328); *PAN4*, encoding a protein containing a PAN4 domain (Pfam: 14295); *PLN03218*, encoding a PLN03218 superfamily protein (Pfam: cl33664) containing multiple PPR motifs.

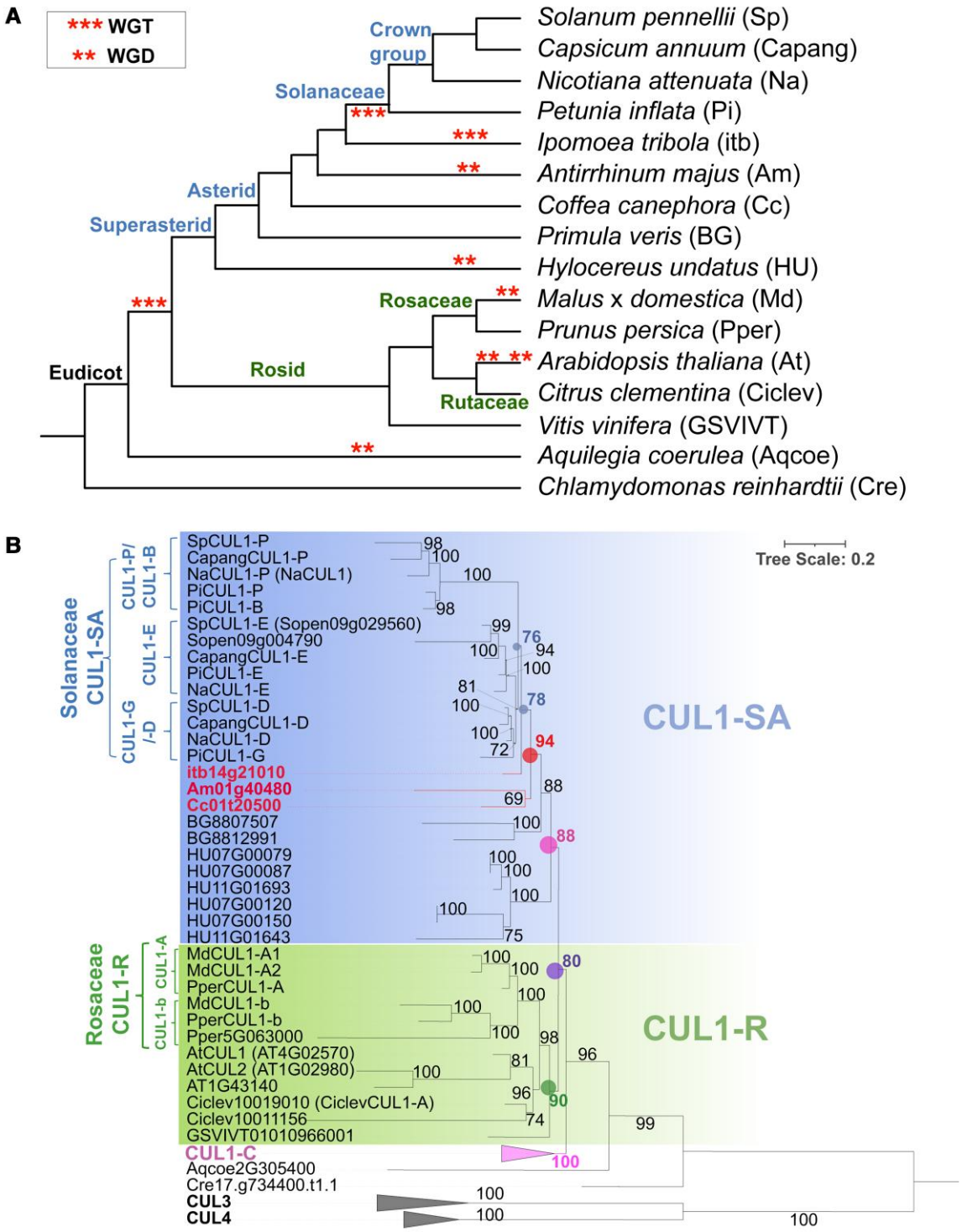

Figure 6 Phylogenetic analysis of Cullin proteins in representative species from various eudicot families. A, Phylogenetic relationship of the species analyzed. *** and ** indicate reported WGT and WGD, respectively, and abbreviations of species names are indicated in parentheses. B, Maximum likelihood phylogenetic analysis of Cullin proteins in the species analyzed. Bootstrap support values (from 1,000 bootstraps) are shown at each node. The nodes containing all Solanaceae CUL1-SA and all Solanaceae CUL1-SA plus the CUL1-SA from *I. tribola* (itb14g21010) are highlighted in blue dots. The node containing all CUL1-SA from the Solanaceae, *I. tribola*, *A. majus*, and *Cof. canephora* is highlighted in red dots. The node containing all CUL1-SA is highlighted in a pink dot, and the node containing all CUL1-R in a green dot. The node containing both CUL1-SA and CUL1-R is highlighted in a purple dot. The scale bar indicates number of substitutions per site. A phylogenetic tree with all branches unfolded is shown in Supplemental Figure S8. It also contains the complete gene accession number of each of the genes whose deduced amino acid sequences were used in the construction of this phylogenetic tree. See Supplemental File 1 for multiple sequence alignment, and Supplemental File 2 for the results of the phylogenetic analysis presented in a Newick file.

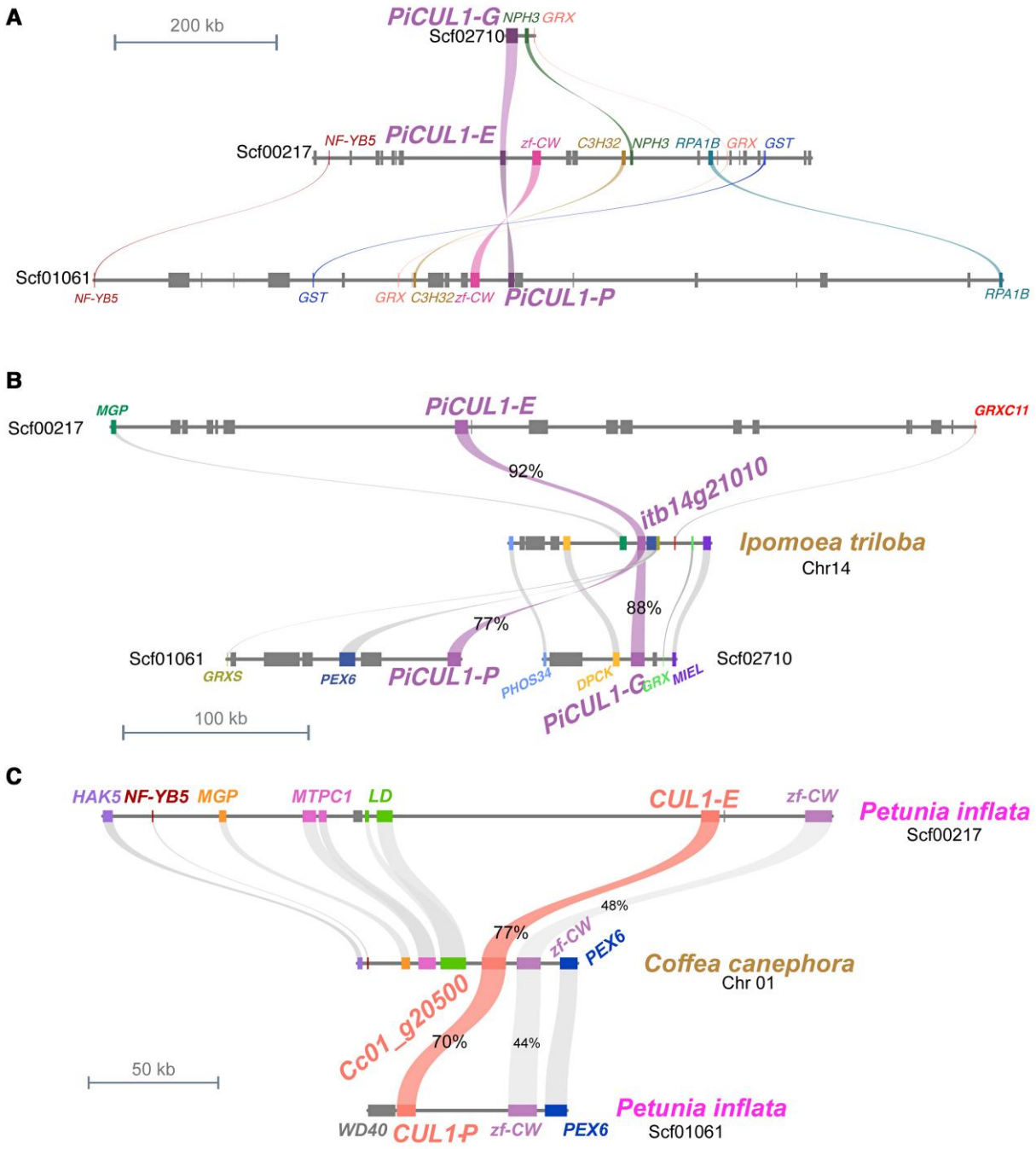

Figure 7 Syntenic relationships among genomic scaffolds containing three *CUL1-SA* genes of *Pe. inflata*, and between genomic regions containing *CUL1-SA* genes in other Asterid species and *CUL1-SA*-containing scaffolds of *Pe. inflata*. A, Synteny between the genes flanking the *CUL1* genes in the scaffolds containing *PiCUL1-P*, *PiCUL1-E*, or *PiCUL1-G*. The synteny is particularly prominent between the *PiCUL1-P*-containing and *PiCUL1-E*-containing scaffolds. B, Location of *itb14g21010*, the only *CUL1-SA* gene in the *I. tribola* genome, and its flanking genes, and comparison with *PiCUL1-P*-, *PiCUL1-E*-, and *PiCUL1-G*-containing scaffolds in the *Pe. inflata* genome. C, Location of a *CUL1-SA* gene, *Cc01t20500*, in the *Cof. canephora* genome and its flanking genes, and comparison with *PiCUL1-P*-containing and *PiCUL1-E*-containing scaffolds in the *Pe. inflata* genome. Gene abbreviations in (A) to (C): *C3H32*, encoding zinc-finger CCCH domain-containing protein 32; *DPCK*, encoding dephospho-CoA kinase; *GRX*, glutaredoxin family genes; *GRXC11*, encoding glutaredoxin-C11; *GRXS2*, encoding a monothiol glutaredoxin S8; *GST*, encoding glutathione S-transferase 7; *HAK5*, encoding High Affinity Potassium (K^+) transporter 5; *LD*, encoding homeobox protein LUMINIDEPENDENS; *MGP*, encoding a C2H2-type zinc-finger protein MAGPIE; *MIEL*, encoding a Myb30-interacting E3 ligase; *MTPC1*, encoding metal tolerance protein C1; *NF-YB5*, encoding nuclear factor Y, Subunit B5; *NPH3*, encoding phototropic-responsive NPH3 family protein; *PHOS34*, encoding universal stress protein PHOS34; *RPA1B*, coding replication protein A 70 kDa DNA-binding subunit B. All other gene abbreviations are listed in the legend to Figure 5.

2016; Zhang et al., 2020). Among these three *CUL1-SA* genes in the Solanaceae, only *CUL1-P* is involved in SI, and it might have undergone another dispersed duplication event that gave rise to *CUL1-B*.

Identification of different evolutionary patterns of SI-specific *CUL1* in the Solanaceae and potentially SI-specific *CUL1* in the Plantaginaceae

Our comprehensive phylogenetic analysis of Cullins in eudicots (Figure 6B; Supplemental Figure S8) also provided us an opportunity to identify which CUL1 protein is involved in S-RNase-based SI in families in which the identity of the CUL1 subunit of SCF^{SLF} complexes was not yet known. For example, previous studies showed that AhSSK1, a pollen-specific SSK1 ortholog in self-incompatible *Antirrhinum hispanicum*, was able to interact with AhSLF proteins in vitro, and thus might serve as the Skp1 subunit of SCF^{SLF} in SI (Huang et al., 2006). However, the identity of the CUL1 subunit(s) of SCF^{SLF} in *Antirrhinum* was not determined. Our phylogenetic analysis of eudicot Cullins suggested that Am01g40480, the only *A. majus* CUL1 in the CUL1-SA clade, was a likely candidate due to its close phylogenetic relationship with the Solanaceae-specific CUL1 clade, to which CUL1-P and CUL1-B belong (Figure 6B). Interestingly, RNA-seq results of various *A. majus* tissues (Li et al., 2019a) showed that, among the three *AmCUL1s* identified, *Am01g40480* was the only one with remarkably high transcript levels in both stamen and pollen (Supplemental Figure S10 and Table S6), further supporting the potential role of this CUL1 as a component of SI-specific SCF^{SLF} complexes in *Antirrhinum*.

Although a whole-genome duplication (WGD) event was proposed to have occurred in the Plantaginaceae 46–49 Mya (Li et al., 2019a, 2019b), only one copy of *Am01g40480* was found in the genome of self-compatible *A. majus*. In the genome of self-incompatible *A. hispanicum* (Zhao et al., 2022), we also found only a single copy of the *Am01g40480* ortholog (*GWHPBFSA004950*), and it was located on Chromosome 1. Interestingly, in both *Antirrhinum* genomes, we found that each genomic region containing the *CUL1-SA* gene on Chromosome 1 shared collinearity with a genomic region on Chromosome 2, but with a large genomic segmental gap (Supplemental Figure S11A), indicating the replacement of the genomic segment containing one duplicated copy of this *CUL1-SA* gene in *Antirrhinum* occurred after the WGD in the Plantaginaceae. This observation of *CUL1-SA* gene loss after WGD in *Antirrhinum* contrasts with the findings in the Solanaceae of the preservation of three *CUL1-SA* genes after WGT and further dedication of one of the genes, *CUL1-P*, specifically to SI (Figure 8). We further analyzed a commercial self-compatible *Antirrhinum* plant and found that *Am01g40480* contained a 4-bp deletion in its coding sequence, resulting in the loss of function of this gene (Supplemental Figure S11B).

To investigate whether the loss of a duplicated copy of *Am01g40480* is specific to *Antirrhinum* in the Plantaginaceae, we analyzed the draft genome of *Collinsia rattanii*, another self-compatible Plantaginaceae species (Frazee et al., 2021) and did not find any *Am01g40480* ortholog (Supplemental Figure S11C). Further syntenic analyses between *A. majus* and *Col. rattanii* revealed that a segment of Chromosome 1 of *A. majus* flanking *Am01g40480* shared a high degree of gene synteny with two scaffolds of the *Col. rattanii* genome. However, no *CUL1* genes were found between the two genes homologous with the genes flanking *Am01g40480* in the *A. majus* genome: the gene encoding a protein containing WD40 motifs and the *zf-CW* gene (Supplemental Figure S11D). These results further revealed the loss of the *CUL1-SA* clade genes in *Col. rattanii*, and this may be related to the loss of SI in this Plantaginaceae species.

Potentially SI-related *CUL1-A*-clade gene in Rosids shares a common origin with SI-related *CUL1* genes in Asterids

Our phylogenetic analysis also suggests that CUL1-SA of Superasterids and CUL1-R of Rosids might share a common ancestor that is distinct from the common ancestor of CUL1-C (Figure 6B; Supplemental Figure S8). Indeed, syntenic analysis between the *Pe. inflata* and peach (*Prunus persica*) genomes revealed that the scaffolds containing *PiCUL1-P*, *PiCUL1-G*, or *PiCUL1-E* shared synteny with a genomic region flanking *PperCUL1-A*, a *CUL1-R* clade gene on Chromosome 8 (Supplemental Figure S12). All the other Rosid species we analyzed also possess a *CUL1-A*-clade gene (Figure 6B; Supplemental Figure S8). In addition, the *CUL1-A*-containing regions in the genomes of peach, apple (*Malus* × *domestica*) and *Citrus clementina* are mostly syntenic, and these regions are also syntenic with one *CUL1-R* clade gene (*GSVIVT01010966001*)-containing region in the genome of grapevine (*Vitis vinifera*) in Rosids (Supplemental Figure S13A).

Interestingly, the CUL1-A-clade protein was proposed to be the major CUL1 component functioning in SI in different Rosid species. For example, the *PperCUL1-A* ortholog in *Prunus avium* (*PavCUL1-A*) was proposed to encode the predominant CUL1 subunit for SCF^{SLFL} and SCF^{SFBL}, both because of its significantly higher transcript level in pollen than that of the *CUL1-C*-clade gene (encoding a CUL1 99.5% identical with PperCUL1-C; formerly named *PavCUL1-B* by Matsumoto et al., 2012 and Matsumoto and Tao, 2016), and because of its ability to interact with PavSSK1, PavSLFLs, and PavSFBLs in vitro (Matsumoto et al., 2012; Matsumoto and Tao, 2019; Li et al., 2020). Moreover, only peptides matching PavCUL1-A, but not CUL1-C-clade proteins, were identified in Co-IP/MS experiments using $PavS_6$-RNase as bait against the germinated pollen extracts from S_1S_4 of *Pr. avium* (Matsumoto and Tao, 2019). In apple, pollen-expressed MdCUL1-A1 interacted with MdSSK1 in in vitro binding assays (Minamikawa et al., 2014). Similarly, the *Citrus reticulata* CUL1-A ortholog, CrCUL1-A (identical in amino acid sequence with CiclevCUL1-A shown in Figure 6B) was found to exhibit preferential expression in pollen compared with other tissues, and to interact with the *Citrus* SSK1 ortholog, CrSKP1-e

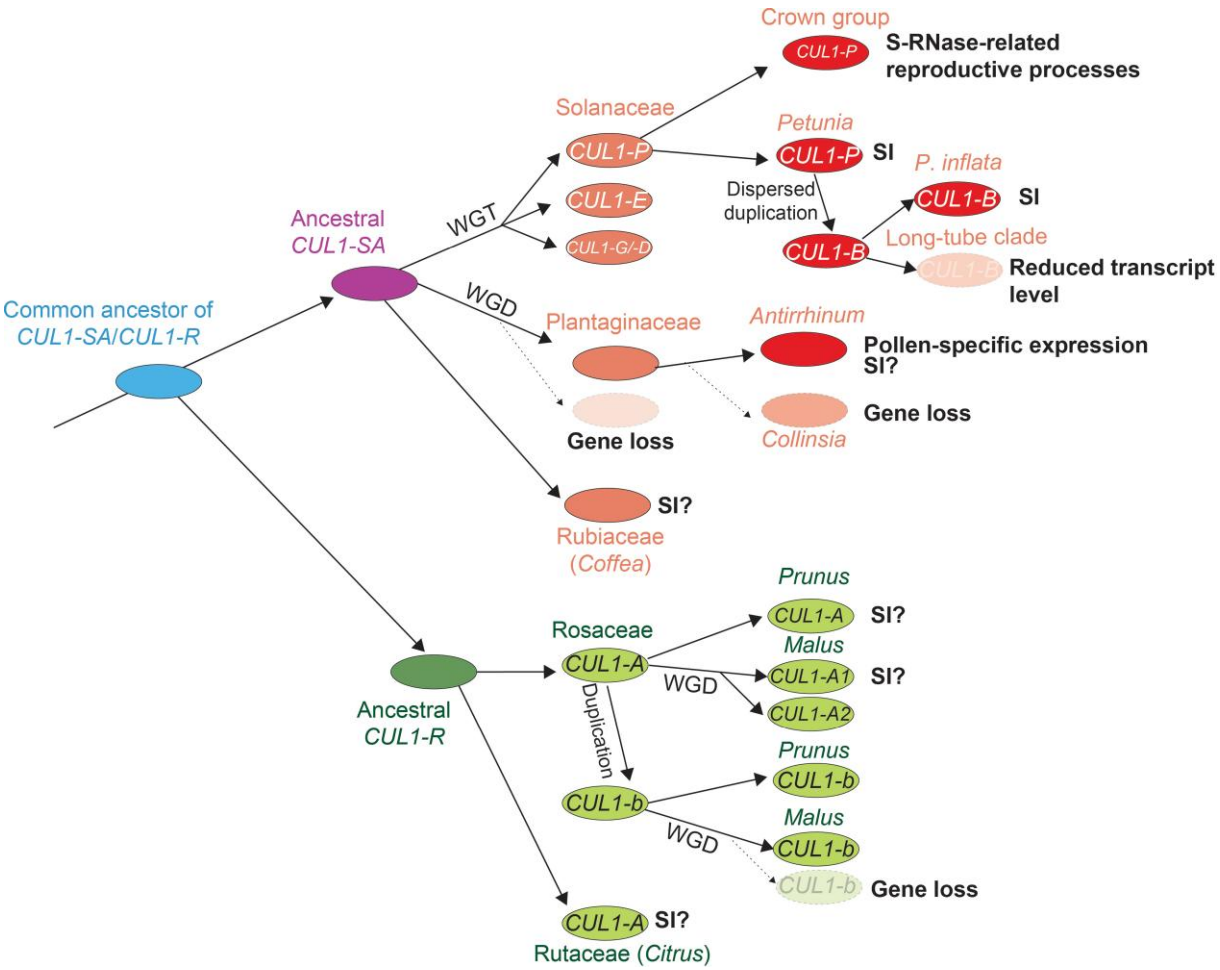

Figure 8 Possible evolutionary patterns of *CUL1* genes involved, or potentially involved, in S-RNase-based SI in different eudicot families. Gene loss or loss-of-function is shown in circles with faded colors. The common ancestor of the genes encoding the CUL1-SA clade proteins and the CUL1-R clade proteins in eudicots is shown in the leftmost circle, which gave rise to both the common ancestor of all *CUL1-SA* genes in superasterid and the common ancestor of all *CUL1-R* genes in Rosid. In the Solanaceae, the ancestral *CUL1-SA* gene triplicated to give rise to three *CUL1* genes, *CUL1-P*, *CUL1-G/CUL1-D*, and *CUL1-E* (the circles under Solanaceae). *CUL1-P* and its dispersed duplicate *CUL1-B* (the circles under Crown group and *Petunia*) were further selected to function in SI, but in the long-tube clade of *Petunia*, transcription of *CUL1-B* is reduced drastically, rendering it nonfunctional in SI. In the Plantaginaceae, one copy of *CUL1-SA* was lost after its WGD. In *Antirrhinum*, the other copy of the *CUL1-SA* gene might be selected to function in SI (the circle under *Antirrhinum*), but in *Collinsia*, this copy of the *CUL1-SA* gene was subsequently lost (the circle above *Collinsia*). In *Coffea* of the Rubiaceae, the *CUL1-SA* gene (the circle above Rubiaceae) was retained, but whether it functions in SI is unknown. In the Rosaceae, the common ancestral *CUL1-R* gene gave rise to *CUL1-A* in both the Rosaceae and *Citrus* of the Rutaceae, and it might be involved in SI in these two families. *CUL1-b* emerged from duplication of *CUL1-A* (the circles under *Prunus* and *Malus*) only in the Rosaceae. In apple, the *Malus*-specific WGD gave rise to two copies of the *CUL1-A* gene, and one of the two copies (*MdCUL1-A*) might be involved in SI. The *Malus* WGD also resulted in duplication of *CUL1-b*, but one copy of *CUL1-b* is truncated, and whether the intact copy of *CUL1-b* functions in SI is unknown.

(Ren et al., 2020). If CUL1-A-clade proteins are indeed the major functional subunit in Rosid $SCF^{SLFL}/^{SFB}/^{SFBB}$ complexes, it is reasonable to predict that the CUL1 proteins dedicated to S-RNase-based SI in Rosids and Asterids also share a common ancestor in eudicots (Figure 8).

In the Rosaceae species we analyzed, there were two clades of CUL1-R, CUL1-A and CUL1-b (originally named CUL1-B by Minamikawa et al., 2014 and Kubo et al., 2016; here we renamed it CUL1-b to distinguish it from *Petunia* CUL1-B we studied). No *CUL1-b* clade gene was found in either the *Ci. clementina* or the grapevine genomes (Figure 6B; Supplemental Figure S8). Also, in both genomes, the regions syntenic with the *PperCUL1-b*-containing regions lacked any *CUL1* genes (Supplemental Figure S13B), indicating that *CUL1-b* is likely a Rosaceae-specific duplication of *CUL1-A*, whereas CUL1-A is the common CUL1-R shared in Rosids (Figure 6B; Supplemental Figure S13A). In apple, although both *MdCUL1-A1* and *MdCUL1-b* are expressed in pollen, MdCUL1-b was unable to interact with MdSSK1 in in vitro binding assays, suggesting that MdCUL-b is not able to form SCF^{SFBB}

complexes (Minamikawa et al., 2014). Therefore, in contrast with the scenario that duplicated copies of *CUL1-P* and *CUL1-B* both function in SI in *Pe. inflata*, in the Rosaceae, it is likely that the duplicated *CUL1-b* is not involved in SI (Figure 8).

In addition, although a recent WGD occurred in the *Malus* genus (Velasco et al., 2010; Li et al., 2019b), the apple genome only encodes one CUL1-b (Figure 6B; Minamikawa et al., 2014). The region containing *PperCUL1-b* in the peach genome was syntenic with two regions in the apple genome, but only the region on Chromosome 6 contained *MdCUL1-b* (*MD06G1052800*), while the other region on Chromosome 4 contained a gene, *MD04G1059200* (Supplemental Figure S13B), that encodes a protein with only the Cullin domain but no Neddylation domain, and thus is unlikely to be fully functional. Therefore, in the apple genome, one duplicated copy of *CUL1-b* appears to have lost its function, while both copies of CUL1-A, containing both the Cullin and Neddylation domains, appear to have potentially retained their function(s).

Discussion

Specific function of CUL1-P and CUL1-B in S-RNase-based reproductive processes

In this work, we have obtained both genetic and biochemical evidence that in *Petunia*, a pair of closely related CUL1 proteins exclusively interact with SSK1 to function as the CUL1 subunit of SCF^{SLF} complexes that mediate the detoxification of nonself S-RNase during cross-compatible pollination. In the Solanaceae, CUL1-P orthologs function not only in SI, but also in other critical reproductive processes that depend on the detoxification of S-RNases by pollen. For example, the pollen-specific *CUL1-P* ortholog in a wild self-incompatible tomato species, *Solanum arcanum*, was shown to be involved in the acceptance of nonself pollen in S-RNase-based interspecific unilateral incompatibility (rejection of pollen from self-compatible species by pistils of self-incompatible species, and acceptance of pollen of self-incompatible species by pistils of self-compatible species; Li and Chetelat, 2010). In *N. attenuata*, a self-compatible wild tobacco species, the pollen-specific CUL1-P ortholog NIATv7_g11649 (named NaCUL1-P in Figure 6B) was shown to interact with NaSSK1 and NaSLF-like1 in yeast two-hybrid assays. Thus, it was suggested to be involved in S-RNase-dependent intraspecific mate selection, which is the preference for certain genotypes of compatible pollen by the pistil (Guo et al., 2019).

Despite the observation that proliferation of *CUL1* genes is common in plants (Figure 6B; Supplemental Figure S8; Kubo et al., 2016; Kim et al., 2018) except for the CUL1-P orthologs in some Solanaceae species (Li and Chetelat, 2014; Kubo et al., 2016), to the best of our knowledge, no other plant CUL1s have been shown to exclusively participate in a specific biological process, or specifically interact with certain Skp1 proteins and/or certain subset of F-box proteins to form SCF complexes. In nonplant model systems such as yeast, fruit fly (*Drosophila melanogaster*), *Caenorhabditis elegans*, mice and human, only one housekeeping CUL1 that can form SCF complexes with a wide range of F-box proteins has been found (reviewed by Sarikas et al., 2011). In the model plant species *Arabidopsis thaliana*, a single CUL1, AtCUL1 (AT4G02570), was shown to form SCF complexes involved in many major hormone signaling pathways, including auxin (SCF^{TIR1}; Gray et al., 1999, 2001; Hellmann et al., 2003), jasmonic acid (SCF^{COI1}; Xu et al., 2002; Thines et al., 2007) and strigolactone ($SCF^{D3/MAX2}$; Stirnberg et al., 2007; Jiang et al., 2013; Zhou et al., 2013; Soundappan et al., 2015). AtCUL1 also interacted with multiple Skp1 and F-box proteins in yeast three-hybrid experiments (Risseeuw et al., 2003) and *in planta* (Gray et al., 1999; del Pozo et al., 2002; Xu et al., 2002). The pleiotropic phenotypes of *AtCUL1* T-DNA knockout mutants (known as *axr6* mutants) also indicate its housekeeping role in Arabidopsis (Shen et al., 2002; Hobbie et al., 2000; Ni et al., 2004; Quint et al., 2005). Similarly, the Skp1 protein ASK1 functions as the predominant Skp1 protein in SCF complexes in Arabidopsis (Yang et al., 1999; Zhao et al., 1999, 2003; Liu et al., 2004; Yapa et al., 2020). Therefore, the SCF^{SLF} complex in pollen of *Pe. inflata* is unique in that both of its Skp1 (PiSSK1; Sun and Kao, 2018) and CUL1 (PiCUL1-P and PiCUL1-B) subunits function specifically in SI. Understanding the biochemical basis for the specific interaction of SSK1 with CUL1-P and CUL1-B in the Solanaceae will provide valuable insights into how the specificity between Skp1 proteins and their cognate CUL1 could be established and maintained. The first step in this endeavor would be to examine the role of the six amino acid residues specific to PiCUL1-P and PiCUL1-B but divergent in other CUL1s that we identified in our structure model of the SCF^{SLF} complex with either PiCUL1-P or PiCUL1-B as the CUL1 subunit (Supplemental Figure S5).

Our findings also highlight the importance of examining the possible specific function of certain nonhousekeeping CUL1s. As some biological processes, such as degradation of S-RNase in pollen, take place in specific tissues or organs, or during specific developmental stages, it would be beneficial for plants to dedicate specific SCF complexes to these processes to avoid interfering with housekeeping functions carried out by a conventional SCF complex. As described below, two examples of such CUL1s with a tissue-specific expression pattern can be found in Arabidopsis. Other than the housekeeping AtCUL1, the Arabidopsis genome encodes two additional CUL1s, AT1G02980 (also known as AtCUL2, but not related to CUL2 in animals found in Elongin B complexes; Sarikas et al., 2011) and AT1G43140 (Shen et al., 2002; Risseeuw et al., 2003; Ren et al., 2005) (Figure 6B). Based on the Arabidopsis BAR eFP database (Honys and Twell, 2003; Klepikova et al., 2016), *AT1G02980* and *AT1G43140* are not expressed in most tissues, but show significantly elevated expression in Stages 12–14 flowers and at the uninucleate microspore stage during pollen development. It would be interesting to examine whether these nonhousekeeping CUL1s have specific functions in related processes such as pollen development in Arabidopsis.

SI to SC transition and loss of functional redundancy of *Petunia* CUL1-P and CUL1-B

In this work, we have also found that the lack of functional redundancy between PhCUL1-P and PhCUL1-B in *Pe. hybrida* might be a result of the drastic reduction of the transcript level of *PhCUL1-B* in the anther, possibly due to the presence of *dPifTP1* DNA transposon sequence in the promoter region of *CUL1-B* inherited from one of its two parental species, *Pe. axillaris* (Figure 4). This result is consistent with the observation that *Pe. axillaris* contributed a much higher proportion of the genes to the *Pe. hybrida* genome than did *Pe. inflata* (Bombarely et al., 2016). Interestingly, the *dPifTP1* DNA transposon sequences in the promoter region of *CUL1-B* were also found in the species of the long-tube clade of *Petunia* (*Pe. axillaris*, *Pe. exserta*, and *Pe. secreta*), but not in *Pe. inflata* of the short-tube clade (Figure 4C). It is thus reasonable to predict that the transcript level of *CUL1-B* in the long-tube clade *Petunia* species is also very low.

Interestingly, it has been reported that almost all species in the short-tube clade of *Petunia* are self-incompatible. Some native populations of *Pe. reitzii* contain both self-incompatible and self-compatible individuals, but self-compatible individuals were thought to have been derived from self-incompatible progenitors via breakdown of SI (Tsukamoto et al., 1998; Reck-Kortmann et al., 2014). On the other hand, the long-tube clade of *Petunia* contains mostly self-compatible species, except for *Pe. axillaris*, which contained many populations of self-incompatible individuals and mixed populations of both self-incompatible and self-compatible individuals (Tsukamoto et al., 1998, 1999; Reck-Kortmann et al., 2014). The drastic reduction of *CUL1-B* transcript level in pollen of most of the long-tube clade species might be related to the widespread loss of SI in this clade. Furthermore, in a self-compatible line of *Pe. hybrida* with the S_mS_m genotype, the pistil does not produce functional S-RNase, and its *PhCUL1-B* carries a 2-bp deletion in the 12th exon (Kubo et al., 2016). This frameshift mutation might be a further evolutionary step towards pseudogenization (i.e. complete loss of function) of *PhCUL1-B* in self-compatible *Pe. hybrida*.

Fixation of loss-of-function mutations in the *CUL1-P* orthologs has been reported to occur after the loss of pistil function in SI during the transition from SI to SC in *Solanum*, possibly reinforcing reproductive isolation between self-incompatible and self-compatible populations. For example, in South American populations of *Solanum habrochaites*, it was reported that loss-of-function mutations of the *CUL1-P* ortholog were only found in the marginal self-compatible populations that lack expression of *S-RNase* in pistils, and that the central (more ancestral) populations that contain both self-incompatible and self-compatible individuals still express functional *CUL1-P* ortholog in pollen (Markova et al., 2016). Due to the presence of the redundant CUL1-P and CUL1-B in *Petunia*, after the loss of pistil SI function during the transition from SI to SC, instead of initial direct pseudogenization of *CUL1-P*, the functional redundancy of CUL1-P and CUL1-B was abolished by first reducing the transcript level of the redundant *CUL1-B* and further mutating this gene in its coding sequence.

On the other hand, in a self-incompatible natural population, loss-of-function mutations in the *CUL1-P* orthologs of *Solanum* (Markova et al., 2017) and in *PiSSK1* of *Pe. inflata* (Sun and Kao, 2018) can be retained through the female side, as these genes are only involved in pollen function in SI, and the pistil SI function is not affected by loss-of-function of these genes. For example, as *Solanum* lacks *CUL1-B*, the *CUL1-P* ortholog is the only *CUL1* involved in cross-compatibility (Li and Chetelat, 2010, 2014). Therefore, in a self-incompatible *Solanum* population, if a plant carries a wild-type allele and a loss-of-function mutant allele of this *CUL1* gene, half of the pollen produced would carry the wild-type allele and the other half would carry the mutant allele, and only the latter would be rejected by normally compatible pistils producing nonself S-RNases. However, the pistil of this plant would function normally in SI and accept wild-type pollen carrying any compatible *S*-haplotype. Thus, the mutant allele of this *CUL1* gene could be passed on to the progeny (Markova et al., 2017).

In the case of self-incompatible *Pe. inflata*, and possibly all the other self-incompatible short-tube *Petunia* species that possess the functionally redundant *CUL1* genes, only when a plant carries loss-of-function mutant alleles of both *CUL1-P* and *CUL1-B*, would the pollen be completely rejected by normally compatible pistils. If a plant carries only a mutant allele of one of the genes, 75% of the pollen produced would still behave normally in SI and be accepted by pistils of self-incompatible plants carrying different *S*-genotypes. Therefore, gene redundancy makes it less likely for pollen produced by a plant to be completely rejected due to *CUL1* mutations, allowing maintenance of cross-compatibility in a self-incompatible *Petunia* population. Because the CUL1 subunit of an SCF complex is the largest in size compared with the other three smaller subunits, it might be more prone to loss-of-function mutations. Therefore, possessing two CUL1 proteins capable of serving as the CUL1 subunit of SCF^{SLF} complexes gives an evolutionary advantage to counteract the higher likelihood of *CUL1* mutations that would affect the assembly of functional SCF^{SLF} complexes required for cross-compatible pollination.

Possible timing of the duplication of *CUL1-P* clade genes in the Solanaceae

In the Solanaceae, *CUL1-B* is only found in *Petunia*; for *Solanum* and *Nicotiana* in the crown-group clade of the Solanaceae, the genomic position corresponding to *CUL1-B* in *Petunia* is occupied by *PLN03218* genes (Figure 5B). In the other Asterid genomes we have analyzed, the genomic regions syntenic with *PiCUL1-B*-containing scaffold do not contain either *CUL1* or *PLN03218* (Figure 5B). The timing of the duplication of *CUL1-P* into *CUL-B* is as yet unknown, but here we envision two possible evolutionary scenarios, illustrated in

Supplemental Figure S14. In the first scenario labeled (1), duplication of *CUL1-P* and transposition of the duplicated copy into its current genomic region occurred early before the split of Petunioideae and the crown group of the Solanaceae (node a, or node b, of the phylogenetic tree); *CUL1-B* was subsequently replaced by *PLN03218* in the common ancestor of the crown group of the Solanaceae (node e), but was retained in Petunioideae, to which the *Petunia* genus belongs. If true, the loss of *CUL1-B* might be a result of a higher degree of gene fractionation (deletion of one copy of duplicated genes; Cheng et al., 2018) in the crown group compared with *Petunia* (Grandont et al., 2016; Bombarely et al., 2016). Alternatively, in the scenario labeled (2), the insertion of *PLN03218* into this region occurred prior to the duplication of *CUL1-B* from *CUL1-P*, and it occurred before the split of Petunioideae and the crown group of the Solanaceae (node a, or node b). Although *PLN03218* was further retained in this genomic region of the crown group of the Solanaceae, duplication of *CUL1-B* from *CUL1-P* replaced *PLN03218* either in the common ancestor of Petunioideae (node c), or in the *Petunia* genus (node d). If this is correct, the duplication event that gave rise to *CUL1-B* might be an evolutionary step towards reinforcement of SI, as SI is widespread in both *Petunia* and other Petunioideae genera, such as *Calibrachoa* (Tsukamoto et al., 2002). To better understand the evolution of the duplicated *CUL1-P* and *CUL1-B* in the Solanaceae, it would be interesting to obtain *CUL1* gene sequences from genome sequences of other genera in Petunioideae, such as *Calibrachoa*, and Solanaceae genera in the clade sister to the clade containing both Petunioideae and the crown group, such as *Salpiglossis* (see the phylogenetic tree in Supplemental Figure S14; Särkinen et al., 2013).

A possible common origin of the SI-related and potentially SI-related *CUL1* genes in eudicots

A common feature of S-RNase-based SI in eudicots is the utilization of pollen-specific F-box proteins (SLFs in the Solanaceae and Plantaginaceae, SLFLs/SFBs in *Prunus*, and SFBB in Malinae of Rosaceae) for pollen specificity in SI. Interestingly, phylogenetic analyses indicated that all these F-box proteins share a common ancestor (Morimoto et al., 2015; Zhao et al., 2022). This raised the possibility that each of the two other SCF complex subunits, Skp1 and CUL1, that are involved in SI in different families of eudicots might also share a common ancestor.

To address the question of whether the CUL1s that function in S-RNase-based SI in eudicots share a common origin, it is necessary to identify the CUL1s involved in S-RNase-based SI in families other than Solanaceae. However, this has not yet been accomplished due to the difficulty of performing reverse genetics experiments in Plantaginaceae and Rosaceae species. In our work, we found that the only copy of the *CUL1-SA* clade gene in the *A. majus* genome also exhibits a pollen-specific expression pattern, suggesting that this CUL1 may function specifically in SI in *Antirrhinum* (Supplemental Figure S10). Further biochemical and genetic experiments are necessary to determine whether this CUL1 interacts with *Antirrhinum* SSK1 in pollen, and whether it is the only CUL1 for the assembly of the SCF^{SLF} complex. If this CUL1 indeed functions in SI, this would indicate that two different families (the Solanaceae and Plantaginaceae) in the Asterids utilize the same clade of CUL1 as the scaffold protein for SCF^{SLF} complexes to function in SI, and that the genes for both these two CUL1 proteins evolved a pollen-specific expression pattern.

In Rosids, both CUL1-R clade proteins (e.g. CUL1-A in *Pr. avium*, MdCUL1-A1 in apple, and CrCUL1-A in *Ci. reticulata*; Matsumoto et al., 2012; Minamikawa et al., 2014; Matsumoto and Tao, 2016, 2019; Ren et al., 2020) and CUL1-C-clade proteins (e.g. PbCUL1 in *Pyrus bretschneideri* and MdCUL1 in apple; Xu et al., 2013; Yuan et al., 2014) have been predicted to serve as the CUL1 subunit in $SCF^{SLFL}/^{SFB}/^{SFBB}$ complexes. However, these predictions of the CUL1s involved in SI in Rosaceae species have all been made based on their ability to interact with SSK1 and SLFL/SFB/SFBB proteins in in vitro experiments, and their expression levels in pollen. It is thus important that in vivo protein–protein interaction and functional assays be performed to obtain direct evidence for the identify the CUL1 subunit of $SCF^{SLFL}/^{SFB}/^{SFBB}$ complexes in Rosids.

If CUL1-A-clade proteins are indeed the major CUL1 subunits of $SCF^{SLFL}/^{SFB}/^{SFBB}$ complexes in Rosids (Matsumoto and Tao, 2016, 2019; Ren et al., 2020), the syntenic relationship between *CUL1-A*-containing genomic regions in the Rosaceae and *CUL1-SA*-containing genomic regions in Asterids (Supplemental Figure S12) would suggest that the *CUL1*s involved in SI in eudicots also share a common ancestor of *CUL1-SA* and *CUL1-R* clade genes. Interestingly, in the Rosaceae, *CUL1-A* genes do not exhibit a pollen-specific expression pattern (Matsumoto et al., 2012; Minamikawa et al., 2014), whereas in *Ci. reticulata* of the Rutaceae, *CrCUL1-A* was shown to be expressed predominantly in pollen (Ren et al., 2020). In both families, the *SSK1* orthologs exhibit a pollen-specific expression pattern (Minamikawa et al., 2014; Matsumoto and Tao, 2016; Ren et al., 2020). Therefore, even if different families in eudicots might utilize CUL1 of the same origin for S-RNase-based SI, the pollen-specific expression pattern of the CUL1 might not be shared by all families.

Materials and methods

Plant materials and growth conditions

Petunia inflata plants of the S_2S_3, S_3S_3, S_7S_7, and $S_{6a}S_{12}$ genotypes were from our laboratory's genetic stock and are available upon demand (Ai et al., 1990; Wang et al., 2001; Sun and Kao, 2013, 2018; Sun et al., 2018). The *As-*S_3/S_3S_3 transgenic plants were identified from selfed progeny of previously generated self-compatible *As-*S_3/S_2S_3 transgenic plants, in which an antisense S_3*-RNase* transgene (*As-*S_3) was used to suppress the production of S_3-RNase in the pistil (Lee et al., 1994; Sun and Kao, 2013, 2018; Sun et al., 2018). Mature *Pe. hybrida* plants were

purchased from a plant nursery in State College, PA, USA, and a mature *A. majus* plant (var. Solstice Purple) was obtained from the Tower Road Landscape Facility at the Pennsylvania State University. The *Pe. inflata* seedlings were grown at 30°C with a light cycle of 16 h under 57 μmol m^{-2} s^{-1} cool white lights (Philips 40-Watt Cool White Linear Fluorescent Light Bulbs). All mature plants were maintained in the Biology (Buckhout) Greenhouse at the Pennsylvania State University, University Park, PA, with the temperature kept at 25°C and a light/dark cycle of 16 h/8 h under a high-pressure sodium light system (1080 Watt PL 2000; P.L. Light Systems).

Generation and characterization of CRISPR/Cas9-mediated gene knockout plants

The CRISPR/Cas9 construct targeting *PiCUL1-P* and the CRISPR/Cas9 construct targeting *PiCUL1-B* (Supplemental Figure S1A) were generated following the protocol reported by Xie et al. (2015), Sun and Kao (2018), and Sun et al. (2018). Briefly, the 20-bp gRNA sequence targeting *PiCUL1-P* (*PPS*) and the 20-bp gRNA sequence targeting *PiCUL1-B* (*BPS*) were separately fused with the same pre-tRNA sequence. Two halves of each tRNA-gRNA fragment were separately synthesized by PCR with Phusion High-Fidelity DNA polymerase (Thermo Fisher Scientific), using the pGTR plasmid (obtained from the Yinong Yang laboratory at the Pennsylvania State University) as template and primers S51AD5-F and S3AD5-R (Supplemental Table S2). The two halves were ligated into a single *PTG* DNA fragment using the Golden Gate Assembly method with restriction enzyme *Bsa*I and T7 DNA ligase (both from New England BioLabs, NEB). Each *PTG* DNA fragment was digested with *Fok*I (NEB) and ligated into *Bsa*I-digested pKSE401 vector (Xing et al., 2014; a gift from Qi-Jun Chen; Addgene plasmid #62202) with T4 DNA ligase (Promega). Each resulting PTG-CRISPR/Cas9 construct was transformed into *Agrobacterium tumefaciens* LBA4404 strain (Invitrogen) via electroporation.

Transformation of wild-type *Pe. inflata* plants of S_2S_3 genotype and extraction of genomic DNA from regenerated plants using DNAZol ES (Molecular Research Center., Inc., MRC) were performed as described by Meng et al. (2011). PCRs for identifying transgenic plants were performed using *Taq* DNA polymerase (NEB), and PCRs for amplifying *PiCUL1-P* and *PiCUL1-B* target regions were performed using Phusion DNA polymerase. PCR products of the *PiCUL1-P* and *PiCUL1-B* target regions were sequenced using Sanger sequencing at the Genomics Core Facility of the Huck Institutes of the Life Sciences at the Pennsylvania State University. If multiple allelic sequences were found from sequencing chromatograms of the PCR products of a particular knockout plant, the PCR products were A-tailed with *Taq* DNA polymerase according to the manufacturer's protocol (NEB), and ligated into pGEM-T Easy vector (Promega) with T4 DNA ligase for further Sanger sequencing of individual clones. For genotyping by restriction enzyme digestion, PCR products were digested at 37°C for 3 h and electrophoresed on 2% agarose gels. All restriction enzymes were purchased from NEB.

Pollination assay and aniline blue staining of pollen tubes in the pistil

Pollination was performed on open flowers, except that pollination of the self-compatible $As\text{-}S_3/S_3S_3$ transgenic plants was performed on flowers 1 day before flower opening, when anthers were not yet dehisced. After all five stamens were removed from each flower, the stigma was pollinated using pollen from mature flowers, and each pollinated pistil (stigma and style) was collected 20 h after pollination for aniline blue staining, as previously described (Sun and Kao, 2018; Sun et al., 2018). The stained pollen tubes in the pistil were observed under the UV lamp of a Nikon Eclipse 90i epifluorescence microscope equipped with a DAPI filter.

cDNA synthesis

Total RNA was extracted from different tissues using the Trizol reagent (MRC). One microgram of total RNA was treated with DNase I (Thermo Fisher Scientific), and reverse transcribed using oligo(dT) and Smart-Scribe reverse transcriptase, following the manufacturer's protocol (Clontech).

Generation of transgenic plants for co-immunoprecipitation

Transgenic plants expressing PiSSK1:FLAG:GFP and Myc:PiCUL1-P were generated by Li et al. (2014, 2016), respectively. To generate transgenic plants expressing Myc:PiCUL1-B or Myc:PhCUL1-B, Phusion DNA polymerase was used both to amplify the full-length *PiCUL1-B* coding sequence from total cDNA of Stage 3 anthers of wild-type S_2S_3 plants and to amplify the full-length *PhCUL1-B* coding sequence from total cDNA of 3-cm anthers of *Pe. hybrida* plants, in both cases using primers *CUL1-B*-Full-F and *CUL1-B*-Full-R. Sequences encoding the *LAT52* promoter of tomato ($LAT52_{pro}$; Twell et al., 1990) used to drive the *Myc:PiCUL1-B* or *Myc:PhCUL1-B* transgene were fused into *Sal*I and *Eco*RI double-digested pBI101 vector (Clontech) using the In-fusion HD Cloning Kit (Takara Bio). The $LAT52_{pro}$*:PhSSK1:FLAG:GFP* plasmid was generated by overlapping PCR using the $LAT52_{pro}$*:PiSSK1:FLAG:GFP* plasmid to convert the codons for serine-78 (S78) and glutamic acid-79 (E79) of PiSSK1 into the codons for glycine and lysine, respectively (corresponding to G78 and K79 of PhSSK1) using the In-fusion HD Cloning Kit. All these plasmids generated were electroporated into *Agrobacterium* LBA4404 strain for transformation of wild-type S_2S_3 plants. PCR was used to identify transgenic plants using *Taq* DNA polymerase (NEB) and primers specific to each transgene (Supplemental Table S2). Double transgenic plants were generated by pollinating immature flower buds of plants in one transgenic line with pollen from plants in another transgenic line, and progeny plants were genotyped using PCR with *Taq* DNA polymerase (NEB).

Co-immunoprecipitation assay

Mature pollen collected from open flowers of each plant was placed in a microfuge tube, resuspended in 1 mL of double

distilled water, and centrifuged at 12,000*g* for 10 min. After the liquid was removed, pollen grains were snap frozen in liquid nitrogen, and then homogenized with a buffer containing 20 mM HEPES, pH 7.5, 150 mM NaCl, 0.05% Tween 20 (v/v), protease inhibitor cocktail (Sigma-Aldrich), and 1 mM phenylmethanesulfonyl fluoride. The homogenized pollen grains were centrifuged at 16,000*g* at 4°C for 15 min, and the supernatant in each tube was kept as the pollen protein extract. For input, each sample of pollen protein extract was diluted in 3x sodium dodecyl sulfate (SDS) sample buffer (180 mM Tris-HCl, pH 6.8, with 30% v/v glycerol, 15% v/v β-mercaptoethanol, 6% w/v SDS, and 0.12% w/v bromophenol blue) and then denatured by heating at 95°C for 10 min. Protein concentrations were determined using the Bio-Rad Protein Assay kit (Bio-Rad). For immunoprecipitation, pollen protein extracts were incubated with 25 µL of equilibrated GFP-Trap® agarose beads (ChromoTek) at 4°C for 2 h with constant rotating, and were subsequently washed using a wash buffer (20 mM HEPES, pH 7.5, 150 mM NaCl, 0.1% v/v Tween 20). Bound proteins were dissociated from agarose beads by heating at 95°C for 10 min in 60 µL 2x SDS sample buffer (diluted from 3x SDS sample buffer with double distilled water; Li et al., 2014, 2016). Both input and Co-IP samples were resolved on 10% SDS-polyacrylamide gels and transferred onto polyvinylidene difluoride membranes (EMD Millipore) for immunoblotting. A mouse monoclonal anti-Myc antibody (clone 4A6, EMD Millipore 05-724, 1:800 dilution) and a horseradish peroxidase (HRP)-conjugated goat anti-mouse IgG (EMD Millipore AP308P, 1:10,000 dilution) were used for anti-Myc immunoblotting. A mouse monoclonal anti-FLAG antibody (clone M2; Sigma-Aldrich F1804, 1:1,000 dilution) and the same HRP-conjugated goat anti-mouse IgG were used for anti-FLAG immunoblotting. Immunoblots were developed with SuperSignal™ West Pico PLUS Chemiluminescent Substrate (Thermo Fisher Scientific) for 5 min, and subsequently visualized using a ChemiDoc XRS Imaging System (Bio-Rad).

Expression and purification of SCF^{SLF} complex subunits in insect cells

For protein expression in insect cells, pFastBac, pFastBac-HTB, and pFastBac-GTE vectors were slightly modified for ligation independent cloning (LIC). Using LIC, coding sequences of *PiCUL1-P* and *PiCUL1-B* were separately cloned into pFastBac-HTB vector, and the coding sequence of *S_2-SLF1* was cloned into the pFastBac-GTE vector. Coding sequences of *PiSSK1* and *PiRBX1* were separately cloned into the pFastBac vector.

His-tagged PiCUL1-B or PiCUL1-P was separately co-expressed with PiRBX1, PiSSK1, and GST-tagged S_2-SLF1 in monolayer Hi5 insect cells (*Trichoplusia ni*; Invitrogen-Thermo Fisher Scientific) using the Bac-to-Bac baculovirus expression system (Invitrogen-Thermo Fisher Scientific). His-tagged PiCUL1-P and PiRBX1 were co-expressed in Hi5 cells to form a binary complex as well. HisPur™ Ni-NTA superflow agarose (Thermo Fisher Scientific) and Pierce™ glutathione agarose (Thermo Fisher Scientific) were used to purify His-tagged PiCUL1-P or PiCUL1-B and GST-tagged S_2-SLF1, respectively, along with their associated protein partners. Ten 150 mm plates of insect cells were grown as a monolayer in Grace's insect medium (Thermo Fisher Scientific) supplemented with 10% fetal bovine serum (GE Healthcare Life Sciences). The cells were harvested 3 days after infection and resuspended in 15 mL lysis buffer (100 mM NaCl and 20 mM HEPES, pH 7.4). Cells were lysed by sonication and subsequently centrifuged at 39,000*g* for 50 min to remove cell debris. Then, 50 µL Ni-NTA or glutathione affinity resin were added into the supernatant and incubated at 4°C for 1 h with gentle mixing. The resins were separated from the supernatant by centrifugation at 700*g* for 15 min and washed with 10 mL lysis buffer. The resins with purified proteins were mixed with SDS sample buffer and heated at 95°C for 10 min. Purified proteins were subsequently resolved on 12% SDS-polyacrylamide gels, and the gels were then stained with Coomassie Brilliant Blue R-250 (Fisher Chemical).

Reverse transcription-quantitative PCR

PowerUp™ SYBR™ Green Master Mix (Thermo Fisher Scientific) was used for RT-qPCR assays, which were performed on an Applied Biosystems™ StepOnePlus™ Real-Time PCR System. Primers used for amplification of each gene analyzed are listed in Supplemental Table S2. The cycling conditions were 95°C for 30 s for initial denaturation, followed by 40 cycles of 95°C for 10 s, 60°C for 20 s, 72°C for 29 s, and then the melt curve stage (95°C for 15 s followed by 60°C for 15 s). A *Petunia ACTIN* gene (Peinf101Scf00999g01020.1 of *Pe. inflata* and its ortholog in *Pe. hybrida*) was used as internal control (Meng et al., 2011; Sun and Kao, 2013; Li et al., 2014). The Δ cycle threshold (ΔCt) method was used to quantify gene expression level (Sun and Kao, 2013).

Identification of amino acid sequences encoded by *Cullin* genes in published or publicly available genome databases

To identify deduced amino acid sequences encoded by *Cullin* genes from the genome databases using the annotated protein sequences available, the deduced amino acid sequence of PiCUL1-C was used to query the protein sequences from each genome sequence database with jackhmmer in HMMER 3.3.2 (Johnson et al., 2010; https://hmmer.org/). Each jackhmmer hit above the default inclusion threshold (*e*-value of 0.001) was then used to query the CDC v3.19 database (Lu et al., 2020) using Batch-CD webtool (https://www.ncbi.nlm.nih.gov/Structure/bwrpsb/bwrpsb.cgi). Only proteins containing both a complete Cullin domain (Pfam: 00888) and a complete Neddylation domain (Pfam: 10557) were used for further phylogenetic analyses. For published

or publicly available genomes with no annotated protein sequences (e.g. *Pe. exserta*, *Pe. secreta*, and *Col. rattanii*), an HMM profile was built using the coding sequences of all five *CUL1* genes of *Pe. inflata*, and this HMM profile was then used to query each genome sequence. The deduced amino acid sequence encoded by each HMM hit was similarly queried against the CDC database. Information for all the genome sequence databases is listed in Supplemental Table S4.

Phylogenetic analyses

Multiple sequence alignments of the amino acid sequences of all Cullin proteins identified from the genome sequence databases of selected species (listed in Supplemental Table S4) were separately generated using MAFFT version 7 with the E-INS-i option (Katoh and Standley, 2013; https://mafft.cbrc.jp/). The alignment used is presented in Supplemental File 1. The maximum likelihood phylogenetic analysis based on each alignment was performed using IQ-TREE web server with 1,000 UltraFast bootstraps with the JTT + I + G4 model (Trifinopoulos et al. 2016; http://iqtree.cibiv.univie.ac.at/), and the results are presented as a machine-readable Newick file in Supplemental File 2. The MAFFT alignment option and model used in IQ-TREE for other phylogenetic analyses in this study are shown in the figures presenting the phylogenetic trees from these analyses. Phylogenetic relationships of species analyzed in this study were constructed using TimeTree (Kumar et al., 2017; http://www.timetree.org/). Phylogenetic trees were visualized and edited using iTOL v6 (Letunic and Bork, 2021; https://itol.embl.de/).

Sequence comparisons

Multiple sequence alignments of deduced amino acid sequences or DNA sequences were performed with MUSCLE (Edgar, 2004; https://www.ebi.ac.uk/Tools/msa/muscle/). Alignment and comparison of sequences in the flanking regions of *CUL1-P* and *CUL1-B* in different *Petunia* species was performed using MAFFT online server (Katoh et al., 2019; https://mafft.cbrc.jp/alignment/server/index.html), and LAST hits generated in MAFFT (Kiełbasa et al., 2011) were plotted as dot plots with a threshold score of 39 ($e = 8.4e\text{-}11$).

Syntenic analyses

Syntenic analyses and visualization were performed using the MCScan pipeline (Tang et al., 2008) in the JCVI python library (https://github.com/tanghaibao/jcvi), using General Feature Format (GFF) files and coding sequence (CDS) files from the genome sequence databases of the species selected, with the exception of *Pe. exserta*. For *Pe. exserta*, as no annotated CDS and GFF files are publicly available, we performed gene annotation of scaffolds containing *CUL1-P* and *CUL1-B* (Scaffold 5 and Scaffold 4, respectively) using WebAUGUSTUS (Hoff and Stanke. 2013; https://bioinf.uni-greifswald.de/webaugustus/), and the output CDS and GFF files were used for MCScan.

Protein structure modeling with AlphaFold

AlphaFold2_advanced in ColabFold (https://colab.research.google.com/github/sokrypton/ColabFold/blob/main/beta/AlphaFold2_advanced.ipynb; Mirdita et al., 2022) was used to predict the structural models of two subcomplexes of PiCUL1-B-PiRBX1 and S_2-SLF1-PiSSK1-PiCUL1-B (the first 390 amino acid residues). The models with the highest ranks were chosen for further analyses. By aligning the above two subcomplexes in the overlapping PiCUL1-B region, the complete SCF^{SLF} complex model of S_2-SLF1-PiSSK1-PiCUL1-B-PiRBX1 was generated. The complete SCF^{SLF} complex model of S_2-SLF1-PiSSK1-PiCUL1-P-PiRBX1 was similarly generated. Each predicted protein structure was visualized in the PyMOL Molecular Graphics System, Version 2.0 Schrödinger, LLC.

Accession numbers

Gene accession numbers for *Pe. inflata*, *Pe. Axillaris*, and *Pe. hybrida CUL1* genes are listed in Supplemental Table S1. Information about *CUL1-P* and *CUL1-B* orthologs identified from *Pe. exserta*, *Pe. secreta*, and *S. chilense* is shown in Supplemental Table S5. The accession numbers of all the genes in syntenic regions analyzed are listed in Supplemental Data Set 1. Additional gene sequence accession numbers in the GenBank/EMBL database analyzed in this study are as follows: *PiSSK1* (JF429902.1), *PhSSK1* (FJ490176.1), *PiRBX1* (DQ250021.1), S_2-*SLF1* (AY500391.1), S_3-*SLF1* (AY500392.2), S_2-*RNase* (AF301533.1), S_3-*RNase* (M67991.2), *dPifTP1* (AB375309.1). The accession number of *Petunia ACTIN* gene (used as internal control gene for RT-qPCR experiments) in the *Pe. inflata* genome sequence database is Peinf101Scf00999g01020.1.

Supplemental data

The following materials are available in the online version of this article.

Supplemental Figure S1. Schematic illustration of transgene constructs used for co-immunoprecipitation to assess interactions of PiCUL1-P, PiCUL1-B, and PhCUL1-B with PiSSK1 and PhSSK1, and for in vitro reconstitution of SCF^{SLF} complexes.

Supplemental Figure S2. Schematic illustration of PTG-CRISPR/Cas9 Ti-plasmid constructs used in this study, and genotyping analyses of *PiCUL1-P* and *PiCUL1-B* single knockout plants in bud-selfed progeny of T_0 plants.

Supplemental Figure S3. Generation of *PiCUL1-P* and *PiCUL1-B* double knockout plants.

Supplemental Figure S4. Transcript levels of *PiCUL1-B* in Stage 2 and Stage 3 anthers of *PiCUL1-P* single knockout plants, as assessed by reverse transcription-quantitative PCR.

Supplemental Figure S5. Six unique residues shared only by PiCUL1-P and PiCUL1-B at the potential interface with PiSSK1 in SCF^{SLF} complexes.

Supplemental Figure S6. Comparisons between coding and noncoding flanking sequences of *CUL1-B* of *Petunia*

inflata and *Petunia axillaris* (A), and between those of *CUL1-P* of *Petunia inflata* and *Petunia axillaris* (B).

Supplemental Figure S7. Similarities between coding and noncoding flanking sequences of *CUL1-P* and *CUL1-B* in *Petunia inflata* (A) and in *Petunia axillaris* (B).

Supplemental Figure S8. Maximum likelihood phylogenetic relationship of all Cullin proteins from various eudicot species analyzed.

Supplemental Figure S9. Syntenic relationships between *PiCUL1-B*-containing scaffold of *Petunia inflata* and genomes of other Asterid species.

Supplemental Figure S10. Transcript levels of four *Antirrhinum majus CUL1* genes in various tissues.

Supplemental Figure S11. Frequent loss of *CUL1-SA* genes in Plantaginaceae genomes.

Supplemental Figure S12. Syntenic relationships between the genomic region containing *CUL1-A* of peach (*PperCUL1-A*) and genomic regions containing *CUL1-SA* genes of *Petunia inflata*.

Supplemental Figure S13. Syntenic relationships between the genomic region containing peach *CUL1-A* (*PperCUL1-A*) or *CUL1-b* (*PperCUL1-b*), and corresponding genomic regions of other Rosid species.

Supplemental Figure S14. Possible evolutionary scenarios for the emergence of *CUL1-B* in the Solanaceae.

Supplemental Table S1. Accession numbers of *Petunia inflata*, *Petunia axillaris*, and *Petunia hybrida CUL1* genes.

Supplemental Table S2. Primers used in this study.

Supplemental Table S3. List of plants that carried CRISPR/Cas9-mediated editing of *PiCUL1-P* and/or *PiCUL1-B* generated in this study.

Supplemental Table S4. Genome sequence databases used in this study.

Supplemental Table S5. Information about *CUL1-P* and *CUL1-B* orthologs identified from *Petunia exserta*, *Petunia secreta*, and *Solanum chilense* genomes.

Supplemental Table S6. Transcript levels of *Antirrhinum majus CUL1* genes obtained from the RNA-seq data.

Supplemental Data Set 1. Gene accession numbers in syntenic regions analyzed in this study.

Supplemental Data Set 2. Results of statistical tests in this work.

Supplemental File 1. Multiple sequence alignment of deduced amino acid sequences of Cullin proteins used in phylogenetic analysis.

Supplemental File 2. Phylogenetic relationship of all eudicot Cullin proteins identified in this study in Newick format.

Acknowledgments

The authors thank Y. Yang and B. Minkenberg for providing the pGTR plasmid and for technical advice on CRISPR/Cas9-mediated genome editing, S. Burghard for greenhouse management, and H. Hao and Y. Lyon for general laboratory and greenhouse help.

Funding

This work was supported by Grants IOS-1645557 and IOS-2138062 from the National Science Foundation to T.H.K. and by Howard Hughes Medical Institute (S.C. and N.Z.).

Conflict of interest statement. None declared.

Author contributions

L.S., S.C., N.Z., and T.H.K. designed the experiments. L.S. and S.C. performed the experiments and analyses. L.S. and T.H.K. wrote the paper.

References

Ai Y, Singh A, Coleman CE, Ioerger TR, Kheyr-Pour A, Kao T-H (1990) Self- incompatibility in *Petunia inflata*: isolation and characterization of cDNAs encoding three *S*-allele-associated proteins. Sex Plant Reprod **3**(2): 130–138

Ban Z, Estelle M (2021) CUL3 E3 ligases in plant development and environmental response. Nat Plants **7**(1): 6–16

Berardi AE, Esfeld K, Jäggi L, Mandel T, Cannarozzi GM, Kuhlemeier C (2021) Complex evolution of novel red floral color in *Petunia*. Plant Cell **33**(7): 2273–2295

Bombarely A, Moser M, Amrad A, Bao M, Bapaume L, Barry CS, Bliek M, Boersma MR, Borghi L, Bruggmann R, et al. (2016) Insight into the evolution of the Solanaceae from the parental genomes of *Petunia hybrida*. Nat Plants **2**(6): 16074

Bombarely A, Rosli HG, Vrebalov J, Moffett P, Mueller LA, Martin GB (2012) A draft genome sequence of *Nicotiana benthamiana* to enhance molecular plant-microbe biology research. Mol Plant Microbe Interact **25**(12): 1523–1530

Brewbaker JL, Natarajan AT (1960) Centric fragments and pollen-part mutation of incompatibility alleles in *Petunia*. Genetics **45**(6): 699–704

Cheng F, Wu J, Cai X, Liang J, Freeling M, Wang X (2018) Gene retention, fractionation and subgenome differences in polyploid plants. Nat Plants **4**(5): 258–268

del Pozo JC, Dharmasiri S, Hellmann H, Walker L, Gray WM, Estelle M (2002) AXR1-ECR1-dependent conjugation of RUB1 to the Arabidopsis Cullin AtCUL1 is required for auxin response. Plant Cell **14**(2): 421–433

de Nettancourt D (2001). Incompatibility and Incongruity in Wild and Cultivated Plants. Springer, Berlin, New York

Edgar RC (2004) MUSCLE: multiple sequence alignment with high accuracy and high throughput. Nucleic Acids Res **32**(5): 1792–1797

Entani T, Kubo KI, Isogai S, Fukao Y, Shirakawa M, Isogai A, Takayama S (2014) Ubiquitin-proteasome-mediated degradation of S-RNase in a solanaceous cross-compatibility reaction. Plant J **78**(6): 1014–1021

Frazee LJ, Rifkin J, Maheepala DC, Grant A-G, Wright S, Kalisz S, Litt A, Spigler R (2021). New genomic resources and comparative analyses reveal differences in floral gene expression in selfing and outcrossing *Collinsia* sister species. G3 **11**(8): jkab177

Fujii S, Kubo K, Takayama S (2016) Non-self and self-recognition models in plant self-incompatibility. Nat Plants **2**(9): 16130

Ganko EW, Meyers BC, Vision TJ (2007) Divergence in expression between duplicated genes in Arabidopsis. Mol Biol Evol **24**(10): 2298–2309

Goldraij A, Kondo K, Lee CB, Hancock CN, Sivaguru M, Vazquez-Santana S, Kim S, Phillips TE, Cruz-Garcia F, McClure B (2006) Compartmentalization of S-RNase and HT-B degradation in self-incompatible *Nicotiana*. Nature **439**(7078): 805–810

Grandont L, Tang H, Johns M, Lyons E, Schranz ME (2016) Incomplete gene fractionation after paleopolyploidy: the first study

case in flowering plants revealed by comparison of the *Petunia axillaris* N. and *Solanum lycopersicum* genomes. Nat Plants **2**(6): 16074

Gray WM, del Pozo JC, Walker L, Hobbie L, Risseeuw E, Banks T, Crosby WL, Yang M, Ma H, Estelle M (1999) Identification of an SCF ubiquitin-ligase complex required for auxin response in *Arabidopsis thaliana*. Genes Dev **13**(13): 1678–1691

Gray WM, Kepinski S, Rouse D, Leyser O, Estelle M (2001) Auxin regulates SCF^{TIR1}-dependent degradation of AUX/IAA proteins. Nature **414**(6861): 271–276

Guo H, Halitschke R, Wielsch N, Gase K, Baldwin IT (2019) Mate selection in self-compatible wild tobacco results from coordinated variation in homologous self-incompatibility genes. Curr Biol **29**(12): 2020–2030.e5

Hellmann H, Hobbie L, Chapman A, Dharmasiri S, Dharmasiri N, del Pozo C, Reinhardt D, Estelle M (2003) Arabidopsis AXR6 encodes CUL1 implicating SCF E3 ligases in auxin regulation of embryogenesis. EMBO J **22**(13): 3314–3325

Hobbie L, McGovern M, Hurwitz LR, Pierro A, Liu NY, Bandyopadhyay A, Estelle M (2000) The *axr6* mutants of *Arabidopsis thaliana* define a gene involved in auxin response and early development. Development **127**(1): 23–32

Hoff KJ, Stanke M (2013) WebAUGUSTUS—a web service for training AUGUSTUS and predicting genes in eukaryotes. Nucleic Acids Res **41**(W1): W123–W128

Honys D, Twell D (2003) Comparative analysis of the Arabidopsis pollen transcriptome. Plant Physiol **132**(2): 640–652

Hosmani PS, Flores-Gonzalez M, van der Geest H, Maumas F, Bakker LV, Schijlen E, van Haarst J, Cordewener J, Sanchez-Perez G, Peters S, et al. (2019). An improved de novo assembly and annotation of the tomato reference genome using single-molecule sequencing, Hi-C proximity ligation and optical maps. bioRxiv. doi: 10.1101/767764

Hua ZH, Kao T-H (2006) Identification and characterization of components of a putative *Petunia* S-locus F-box-containing E3 ligase complex involved in S-RNase-based self-incompatibility. Plant Cell **18**(10): 2531–2553

Hua ZH, Meng XY, Kao T-H (2007) Comparison of *Petunia inflata* S-Locus F-Box protein (Pi SLF) with Pi SLF–Like proteins reveals its unique function in S-RNase–based self-incompatibility. Plant Cell **19**(11): 3593–3609

Huang J, Zhao L, Yang Q, Xue Y (2006) AhSSK1, a novel SKP1-like protein that interacts with the S-locus F-box protein SLF. Plant J **46**(5): 780–793

Huang S, Lee HS, Karunanandaa B, Kao T-H (1994) Ribonuclease activity of *Petunia inflata* S proteins is essential for rejection of self-pollen. Plant Cell **6**(7): 1021–1028

Jiang L, Liu X, Xiong G, Liu H, Chen F, Wang L, Meng X, Liu G, Yu H, Yuan Y, et al. (2013) DWARF 53 Acts as a repressor of strigolactone signalling in rice. Nature **504**(7480): 401–405

Johnson LS, Eddy SR, Portugaly E (2010) Hidden Markov model speed heuristic and iterative HMM search procedure. BMC Bioinformatics **11**(1): 431

Katoh K, Rozewicki J, Yamada KD (2019) MAFFT Online service: multiple sequence alignment, interactive sequence choice and visualization. Brief Bioinform **20**(4): 1160–1166

Katoh K, Standley DM (2013) MAFFT Multiple sequence alignment software version 7: improvements in performance and usability. Mol Biol Evol **30**(4): 772–780

Kiełbasa SM, Wan R, Sato K, Horton P, Frith MC (2011) Adaptive seeds tame genomic sequence comparison. Genome Res **21**(3): 487–493

Kim S-H, Woo O-G, Jang H, Lee J-H (2018) Characterization and comparative expression analysis of *CUL1* genes in rice. Genes Genom **40**(3): 233–241

Klepikova AV, Kasianov AS, Gerasimov ES, Logacheva MD, Penin AA (2016) A high resolution map of the *Arabidopsis thaliana* developmental transcriptome based on RNA-seq profiling. Plant J **88**(6): 1058–1070

Kubo K, Entani T, Takara A, Wang N, Fields AM, Hua ZH, Toyoda M, Kawashima S, Ando T, Isogai A, et al. (2010) Collaborative non-self recognition system in S-RNase-based self-incompatibility. Science **330**(6005): 796–799

Kubo K, Paape T, Hatakeyama M, Entani T, Takara A, Kajihara K, Tsukahara M, Shimizu-Inatsugi R, Shimizu KK, Takayama S (2015) Gene duplication and genetic exchange drive the evolution of S-RNase-based self-incompatibility in *Petunia*. Nat Plants **1**(1): 14005

Kubo K, Tsukahara M, Fujii S, Murase K, Wada Y, Entani T, Iwano M, Takayama S (2016) Cullin1-P is an essential component of non-self recognition system in self-incompatibility in *Petunia*. Plant Cell Physiol **57**(11): 2403–2416

Kumar S, Stecher G, Suleski M, Hedges SB (2017) Timetree: a resource for timelines, timetrees, and divergence times. Mol Biol Evol **34**(7): 1812–1819

Lee HS, Huang S, Kao T-H (1994) S proteins control rejection of incompatible pollen in *Petunia inflata*. Nature **367**(6463): 560–563

Letunic I, Bork P (2021) Interactive tree of life (iTOL) v5: an online tool for phylogenetic tree display and annotation. Nucleic Acids Res **49**-(W1): W293–W296

Li H, Huang C-H, Ma H (2019a) Whole-genome duplications in pear and apple. *In* TP Genome, SS Korban, eds, Compendium of Plant Genomes. Springer International Publishing, Cham, pp. 279–299

Li M, Zhang D, Gao Q, Luo Y, Zhang H, Ma B, Chen C, Whibley A, Zhang Y, Cao Y, et al. (2019b) Genome structure and evolution of *Antirrhinum majus* L. Nat Plants **5**(2): 174–183

Li S, Sun P, Williams JS, Kao T-H (2014) Identification of the self-incompatibility locus F-box protein-containing complex in *Petunia inflata*. Plant Reprod **27**(1): 31–45

Li S, Williams JS, Sun P, Kao T-J (2016) All 17 types of S-locus F-box proteins of S_2- and S_3-haplotypes of *Petunia inflata* are assembled into similar SCF complexes with specific function in self-incompatibility. Plant J **87**(6): 606–616

Li W, Chetelat RT (2010) A pollen factor linking inter- and intraspecific pollen rejection in tomato. Science **330**(6012): 1827–1830

Li W, Chetelat RT (2014) The role of a pollen-expressed Cullin1 protein in gametophytic self-incompatibility in *Solanum*. Genetics **196**(2): 439–442

Li Y, Duan X, Wu C, Yu J, Liu C, Wang J, Zhang X, Yan G, Jiang F, Li T, et al. (2020) Ubiquitination of S_4-RNase by S-locus F-box Like2 contributes to self-compatibility of sweet cherry 'Lapins'. Plant Physiol **184**(4): 1702–1716

Liang M, Cao Z, Zhu A, Liu Y, Tao M, Yang H, Xu Q, Wang S, Liu J, Li Y, et al. (2020) Evolution of self-compatibility by a mutant S_m-*RNase* in citrus. Nat Plants **6**(2): 131–142

Liu F, Ni W, Griffith ME, Huang Z, Chang C, Peng W, Ma H, Xie D (2004) The *ASK1* and *ASK2* genes are essential for Arabidopsis early development. Plant Cell **16**(1): 5–20

Liu W, Fan J, Li J, Song Y, Li Q, Zhang Y, Xue Y (2014) SCF^{SLF}-mediated cytosolic degradation of S-RNase is required for cross-pollen compatibility in S-RNase-based self-incompatibility in *Petunia hybrida*. Front Genet **5**: 228

Lu S, Wang J, Chitsaz F, Derbyshire MK, Geer RC, Gonzales NR, Gwadz M, Hurwitz DI, Marchler GH, Song JS, et al. (2020) CDD/SPARCLE: the conserved domain database in 2020. Nucleic Acids Res **48**(D1): D265–D268

Luu DT, Qin X, Morse D, Cappadocia M (2000) S-RNase uptake by compatible pollen tubes in gametophytic self-incompatibility. Nature **407**(6804): 649–651

Markova DN, Petersen JJ, Qin X, Short DR, Valle MJ, Tovar-Méndez A, McClure BA, Chetelat RT (2016) Mutations in two pollen self-incompatibility factors in geographically marginal populations of *Solanum habrochaites* impact mating system transitions and reproductive isolation. Am J Bot **103**(10): 1847–1861

Markova DN, Petersen JJ, Yam SE, Corral A, Valle MJ, Li W, Chetelat RT (2017) Evolutionary history of two pollen self-incompatibility

factors reveals alternate routes to self-compatibility within *Solanum*. Am J Bot **104**(12): 1904–1919

Matsubara K, Shimamura K, Kodama H, Kokubun H, Watanabe H, Basualdo IL, Ando T (2008) Green corolla segments in a wild *Petunia* species caused by a mutation in *FBP2*, a *SEPALLATA*-like MADS box gene. Planta **228**(3): 401

Matsumoto D, Tao R (2016) Recognition of a wide-range of S-RNases by *S* locus F-box like 2, a general-inhibitor candidate in the *Prunus*-specific S-RNase-based self-incompatibility system. Plant Mol Biol **91**(4–5): 459–469

Matsumoto D, Tao R (2019) Recognition of S-RNases by an *S* locus F-box like protein and an *S* haplotype-specific F-box like protein in the *Prunus*-specific self-incompatibility system. Plant Mol Biol **100**(4–5): 367–378

Matsumoto D, Yamane H, Abe K, Tao R (2012) Identification of a Skp1-like protein interacting with SFB, the pollen *S* determinant of the gametophytic self-incompatibility in *Prunus*. Plant Physiol **159**(3): 1252–1262

Meng X, Hua Z, Sun P, Kao T-H (2011) The amino terminal F-box domain of *Petunia inflata* S-locus F-box protein is involved in the S-RNase-based self-incompatibility mechanism. AoB Plants **2011**: plr016

Minamikawa MF, Koyano R, Kikuchi S, Koba T, Sassa H (2014) Identification of SFBB-containing canonical and noncanonical SCF complexes in pollen of apple (*Malus* × *domestica*). PLoS One **9**(5): e97642

Mirdita M, Schütze K, Moriwaki Y, Heo L, Ovchinnikov S, Steinegger M (2022) Colabfold: making protein folding accessible to all. Nat Methods;**19**:679–682

Moore RC, Purugganan MD (2003) The early stages of duplicate gene evolution. Proc Natl Acad Sci U S A **100**(26): 15682–15687

Morimoto T, Akagi T, Tao R (2015) Evolutionary analysis of genes for S-RNase-based self-incompatibility reveals *S* locus duplications in the ancestral Rosaceae. Hortic J **84**(3): 233–242

Mu JH, Lee HS, Kao T-H (1994) Characterization of a pollen-expressed receptor-like kinase gene of *Petunia inflata* and the activity of its encoded kinase. Plant Cell **6**(5): 709–721

Murfett J, Atherton TL, Mou B, Gasser CS, McClure BA (1994) S-RNase expressed in transgenic *Nicotiana* causes *S*-allele-specific pollen rejection. Nature **367**(6463): 563–566

Ni W, Xie D, Hobbie L, Feng B, Zhao D, Akkara J, Ma H (2004) Regulation of flower development in Arabidopsis by SCF complexes. Plant Physiol **134**(4): 1574–1585

Olmstead RG, Bohs L, Migid HA, Santiago-Valentin E, Garcia VF, Collier SM (2008) A molecular phylogeny of the Solanaceae. Taxon **57**(4): 1159–1181

Qiao X, Li Q, Yin H, Qi K, Li L, Wang R, Zhang S, Paterson AH (2019) Gene duplication and evolution in recurring polyploidization-diploidization cycles in plants. Genome Biol **20**(1): 38

Quint M, Ito H, Zhang W, Gray WM (2005) Characterization of a novel temperature-sensitive allele of the CUL1/AXR6 subunit of SCF ubiquitin-ligases. Plant J **43**(3): 371–383

Reck-Kortmann M, Silva-Arias GA, Segatto ALA, Mäder G, Bonatto SL, de Freitas LB (2014) Multilocus phylogeny reconstruction: new insights into the evolutionary history of the genus *Petunia*. Mol Phylogenet Evol **81**: 19–28

Ren C, Pan J, Peng W, Genschik P, Hobbie L, Hellmann H, Estelle M, Gao B, Peng J, Sun C, et al. (2005) Point mutations in Arabidopsis *Cullin1* reveal its essential role in jasmonate response. Plant J **42**(4): 514–524

Ren Y, Hua Q, Pan J, Zhang Z, Zhao J, He X, Qin Y, Hu G (2020) SKP1-like protein, CrSKP1-e, interacts with pollen-specific F-box proteins and assembles into SCF-type E3 complex in 'Wuzishatangju' (*Citrus reticulata* Blanco) pollen. PeerJ **8**: e10578

Risseeuw EP, Daskalchuk TE, Banks TW, Liu E, Cotelesage J, Hellmann H, Estelle M, Somers DE, Crosby WL (2003) Protein interaction analysis of SCF ubiquitin E3 ligase subunits from Arabidopsis. Plant J **34**(6): 753–767

Sarikas A, Hartmann T, Pan Z-Q (2011) The cullin protein family. Genome Biol **12**(4): 220

Särkinen T, Bohs L, Olmstead RG, Knapp S (2013) A phylogenetic framework for evolutionary study of the nightshades (Solanaceae): a dated 1000-tip tree. BMC Evol Biol **13**(1): 214

Shen W-H, Parmentier Y, Hellmann H, Lechner E, Dong A, Masson J, Granier F, Lepiniec L, Estelle M, Genschik P (2002) Null mutation of *AtCUL1* causes arrest in early embryogenesis in Arabidopsis. Mol Bio Cell **13**(6): 1916–1928

Sierro N, Battey JN, Ouadi S, Bovet L, Goepfert S, Bakaher N, Peitsch MC, Ivanov NV (2013) Reference genomes and transcriptomes of *Nicotiana sylvestris* and *Nicotiana tomentosiformis*. Genome Biol **14**(6): R60

Sijacic P, Wang X, Skirpan AL, Wang Y, Dowd PE, McCubbin AG, Huang S, Kao T-H (2004) Identification of the pollen determinant of S-RNase-mediated self-incompatibility. Nature **429**(6989): 2–5

Soundappan I, Bennett T, Morffy N, Liang Y, Stanga JP, Abbas A, Leyser O, Nelson DC (2015) SMAX1-LIKE/D53 Family members enable distinct MAX2-dependent responses to strigolactones and karrikins in Arabidopsis. Plant Cell **27**(11): 3143–3159

Stam R, Nosenko T, Hörger AC, Stephan W, Seidel M, Kuhn JMM, Haberer G, Tellier A (2019) The de novo reference genome and transcriptome assemblies of the wild tomato species *Solanum chilense* highlights birth and death of NLR genes between tomato species. G3 **9**(12): 3933–3941

Stirnberg P, Furner IJ, Ottoline Leyser HM (2007) MAX2 participates in an SCF complex which acts locally at the node to suppress shoot branching. Plant J **50**(1): 80–94

Stout AB, Chandler C (1941) Change from self-incompatibility to self-compatibility accompanying change from diploidy to tetraploidy. Science **94**(2431): 118

Stout AB, Chandler C (1942) Hereditary transmission of induced tetraploidy and compatibility in fertilization. Science **96**(2489): 257–258

Sun L, Kao T-H (2018) CRISPR/Cas9-mediated knockout of *PiSSK1* reveals essential role of S-locus F-box protein-containing SCF complexes in recognition of non-self S-RNases during cross-compatible pollination in self-incompatible *Petunia inflata*. Plant Reprod **31**(2): 129–143

Sun L, Williams JS, Li S, Wu L, Khatri WA, Stone PG, Keebaugh MD, Kao T-H (2018) S-locus F-box proteins are solely responsible for S-RNase-based self-incompatibility of *Petunia* pollen. Plant Cell **30**-(12): 2959–2972

Sun P, Kao T-H (2013) Self-incompatibility in *Petunia inflata*: the relationship between a self-incompatibility locus F-box protein and its non-self S-RNases. Plant Cell **25**(2): 470–485

Tang H, Bowers JE, Wang X, Ming R, Alam M, Paterson AH (2008) Synteny and collinearity in plant genomes. Science **320**(5875): 486–488

Thines B, Katsir L, Melotto M, Niu Y, Mandaokar A, Liu G, Nomura K, He SY, Howe GA, Browse J (2007) JAZ Repressor proteins are targets of the SCF^{COI1} complex during jasmonate signalling. Nature **448**-(7154): 661–665

Trifinopoulos J, Nguyen L-T, von Haeseler A, Minh BQ (2016) W-IQ-TREE: a fast online phylogenetic tool for maximum likelihood analysis. Nucleic Acids Res **44**(W1): W232–W235

Tsukamoto T, Ando T, Kokubun H, Watanabe H, Masada M, Zhu X, Marchesi E, Kao T-H (1999) Breakdown of self-incompatibility in a natural population of *Petunia axillaris* (Solanaceae) in Uruguay containing both self-incompatible and self-compatible plants. Sexual Plant Reprod **12**(1): 6–13

Tsukamoto T, Ando T, Kokubun H, Watanabe H, Tanaka RU, Hashimoto G, Marchesi E, Kao T-H (1998). Differentiation in the status of self-incompatibility among all natural taxa of *Petunia* (Solanaceae). Acta Phytotax Geobot **49**(2): 115–133

Tsukamoto T, Ando T, Watanabe H, Kokubun H, Hashimoto G, Sakazaki U, Suárez E, Marchesi E, Oyama K, Kao T-H (2002) Differentiation in the status of self-incompatibility among *Calibrachoa* species (Solanaceae). J Plant Res **115**(3): 185–193

Twell D, Yamaguchi J, McCormick S (1990) Pollen-specific gene expression in transgenic plants: coordinate regulation of two different tomato gene promoters during microsporogenesis. Development **109**(3): 705–713

Velasco R, Zharkikh A, Affourtit J, Dhingra A, Cestaro A, Kalyanaraman A, Fontana P, Bhatnagar SK, Troggio M, Pruss D, et al. (2010) The genome of the domesticated apple (*Malus* × *domestica* Borkh). Nat Genet **42**(10): 833–839

Wang X, Hughes AL, Tsukamoto T, Ando T, Kao T-H (2001) Evidence that intragenic recombination contributes to allelic diversity of the *S-RNase* gene at the self-incompatibility (*S*) locus in *Petunia inflata*. Plant Physiol **125**(2): 1012–1022

Wang Y, Ficklin SP, Wang X, Feltus FA, Paterson AH (2016) Large-scale gene relocations following an ancient genome triplication associated with the diversification of core eudicots. PLoS One **11**(5): e0155637

Williams JS, Der JP, DePamphilis CW, Kao T-H (2014a). Transcriptome analysis reveals the same 17 *S-Locus F-Box* genes in two haplotypes of the self-incompatibility locus of *Petunia inflata*. Plant Cell **26**(7): 2873–2888

Williams JS, Natale CA, Wang N, Li S, Brubaker TR, Sun P, Kao T-H (2014b) Four previously identified *Petunia inflata S-Locus F-box* genes are involved in pollen specificity in self-incompatibility. Mol Plant **7**(3): 567–569

Wu L, Williams JS, Sun L, Kao T-H (2020) Sequence analysis of the *Petunia inflata S*-locus region containing 17 *S-Locus F-Box* genes and the *S-RNase* gene involved in self-incompatibility. Plant J **104**(5): 1348–1368

Wu L, Williams JS, Wang N, Khatri WA, San Román D, Kao T-H (2018) Use of domain-swapping to identify candidate amino acids involved in differential interactions between two allelic variants of type-1 S-locus F-box protein and S_3-RNase in *Petunia inflata*. Plant Cell Physiol **59**(2): 234–247

Xie K, Minkenberg B, Yang Y (2015) Boosting CRISPR/Cas9 multiplex editing capability with the endogenous tRNA-processing system. Proc Natl Acad Sci U S A **112**(11): 3570–3575

Xing HL, Dong L, Wang ZP, Zhang HY, Han CY, Liu B, Wang XC, Chen QJ (2014) A CRISPR/Cas9 toolkit for multiplex genome editing in plants. BMC Plant Biol **14**(1): 327

Xu C, Li M, Wu J, Guo H, Li Q, Zhang Y, Chai J, Li T, Xue Y (2013) Identification of a canonical SCF^{SLF} complex involved in S-RNase-based self-incompatibility of *Pyrus* (Rosaceae). Plant Mol. Biol **81**(3): 245–257

Xu L, Liu F, Lechner E, Genschik P, Crosby WL, Ma H, Peng W, Huang D, Xie D (2002) The SCF^{COI1} ubiquitin-ligase complexes are required for jasmonate response in Arabidopsis. Plant Cell **14**(8): 1919–1935

Xu S, Brockmöller T, Navarro-Quezada A, Kuhl H, Gase K, Ling Z, Zhou W, Kreitzer C, Stanke M, et al. (2017) Wild tobacco genomes reveal the evolution of nicotine biosynthesis. Proc Natl Acad Sci U S A **114**(23): 6133–6138

Yang M, Hu Y, Lodhi M, McCombie WR, Ma H (1999) The Arabidopsis *SKP1-LIKE1* gene is essential for male meiosis and may control homologue separation. Proc Natl Acad Sci U S A **96**-(20): 11416–11421

Yapa MM, Yu P, Liao F, Moore AG, Hua Z (2020) Generation of a fertile *ask1* mutant uncovers a comprehensive set of SCF-mediated intracellular functions. Plant J **104**(2): 493–509

Yuan H, Meng D, Gu Z, Li W, Wang A, Yang Q, Zhu Y, Li T (2014). A novel gene, MdSSK1, as a component of the SCF complex rather than MdSBP1 can mediate the ubiquitination of S-RNase in apple. J Exp Bot **65**(12): 3121–3131

Zhang C, Zhang T, Luebert F, Xiang Y, Huang C-H, Hu Y, Rees M, Frohlich MW, Qi J, Weigend M, et al. (2020) Asterid phylogenomics/phylotranscriptomics uncover morphological evolutionary histories and support phylogenetic placement for numerous whole-genome duplications. Mol Biol Evol **37**(11): 3188–3210

Zhao D, Ni W, Feng B, Han T, Petrasek MG, Ma H (2003) Members of the Arabidopsis *SKP1-like* gene family exhibit a variety of expression patterns and may play diverse roles in Arabidopsis. Plant Physiol **133**(1): 203–217

Zhao D, Yang M, Solava J, Ma H (1999) The *ASK1* gene regulates development and interacts with the *UFO* gene to control floral organ identity in Arabidopsis. Dev Genet **25**(3): 209–223

Zhao H, Zhang Y, Zhang H, Song Y, Zhao F, Zhang Y, Zhu S, Zhang H, Zhou Z Guo H, et al. (2022) Origin, loss, and regain of self-incompatibility in angiosperms. Plant Cell **34**(1): 579–596

Zhao L, Huang J, Zhao Z, Li Q, Sims TL, Xue Y (2010) The Skp1-like protein SSK1 is required for cross-pollen compatibility in S-RNase-based self-incompatibility. Plant J **62**(1): 52–63

Zheng N, Schulman BA, Song L, Miller JJ, Jeffrey PD, Wang P, Chu C, Koepp DM, Elledge SJ, Pagano M, et al. (2002) Structure of the Cul1-Rbx1-Skp1-F box^{Skp2} SCF ubiquitin ligase complex. Nature **416**-(6882): 703–709

Zhou F, Lin Q, Zhu L, Ren Y, Zhou K, Shabek N, Wu F, Mao H, Dong W, Gan L, et al. (2013) D14–SCF^{D3}-dependent degradation of D53 regulates strigolactone signaling. Nature **504**(7480): 406–410